NACA

RESEARCH MEMORANDUM

INVESTIGATION OF WING-TIP AILERONS ON A 51.3° SWEPTBACK WING AT TRANSONIC SPEEDS BY THE TRANSONIC-BUMP METHOD

By William C. Moseley, Jr., and James M. Watson

Langley Aeronautical Laboratory
Langley Field, Va.

NATIONAL ADVISORY COMMITTEE FOR AERONAUTICS

WASHINGTON
November 26, 1951

NATIONAL ADVISORY COMMITTEE FOR AERONAUTICS

RESEARCH MEMORANDUM

INVESTIGATION OF WING-TIP AILERONS ON A 51.3° SWEPTBACK WING AT TRANSONIC SPEEDS BY THE TRANSONIC-BUMP METHOD

By William C. Moseley, Jr., and James M. Watson

SUMMARY

An investigation to determine the aerodynamic characteristics of deflectable wing-tip ailerons on a sweptback wing was made in the Langley high-speed 7- by 10-foot tunnel by means of the transonic-bump technique. The basic wing used in this investigation had 51.3° sweepback at the leading edge, an aspect ratio of 2.87, and a taper ratio of 0.51. Three ailerons were investigated, one with the basic-wing plan form and two with an extended-tip plan form. The aileron as tested on the basic wing was triangular in plan form and was deflected about a hinge axis normal to the leading edge of the wing. With the extended-tip-wing plan form, one aileron was obtained by deflecting the triangular extended-tip area about a spanwise axis through the 0.50-tip-chord station of the basic wing, while the other, a trapezoidal aileron, was obtained by deflecting the area of the wing aft of a spanwise axis through the 0.50-tip-chord station of the basic wing. The Reynolds number of the tests varied from about 1,000,000 to about 1,450,000.

The data indicated that either aileron tested with the extended-tip-wing plan form provided lateral control over the entire Mach number range investigated, except possibly at very high angles of attack. The aileron within the basic-wing plan form provided control up to a Mach number of 0.90 but had large losses in control effectiveness between Mach numbers of 0.90 and 1.03.

INTRODUCTION

The National Advisory Committee for Aeronautics is currently making extensive investigations of various devices in an attempt to find one that will provide adequate lateral control throughout the speed range. One such device, the deflectable wing-tip aileron, has been investigated and found adequate at low speeds (references 1 to 3). A preliminary investigation (reference 4) of a triangular wing-tip aileron on a 42° sweptback wing has indicated that the extended-tip type of lateral-control device holds promise at both subsonic and transonic speeds. The present investigation, utilizing the transonic-bump method, was made in the Langley high-speed 7- by 10-foot tunnel to evaluate the lateral control characteristics of several tip ailerons on a 51.3° sweptback wing through the transonic speed range. Three ailerons were investigated: one was a wing tip deflectable about an axis normal to the leading edge (reference 1); one was a triangular tip added to the basic wing (references 2 to 4); and the third, utilizing the extended-tip area, was a trapezoidal-shaped trailing-edge aileron obtained by deflecting the area rearward of a spanwise axis through the 0.50-tip-chord station of the basic wing.

COEFFICIENTS AND SYMBOLS

C_L	lift coefficient (Twice lift of semispan model/qS)
C_D	drag coefficient (Twice drag of semispan model/qS)
C_m	pitching-moment coefficient referred to $0.25\bar{c}$ (Twice pitching moment of semispan model/$qS\bar{c}$)
C_n	yawing-moment coefficient, one control deflected (N/qSb)
C_l	rolling-moment coefficient, one control deflected (L/qSb)
ΔC_D	incremental drag coefficient resulting from deflection of one aileron
q	effective dynamic pressure over span of model, pounds per square foot $\left(\frac{1}{2}\rho V^2\right)$
S	twice wing area of semispan model; for basic wing, 0.2064 square foot, and for wing with extended tip, 0.2328 square foot
b	twice semispan of model; for basic wing, 0.769 foot, and for wing with extended tip, 1.061 feet

$\bar{c}$ mean aerodynamic chord $\left(\frac{2}{S}\int_0^{b/2} c^2 dy\right)$; for basic wing, 0.278 foot, and for wing with extended tip, 0.260 foot

c local wing chord, feet

y spanwise distance from plane of symmetry, feet

ρ mass density of air, slugs per cubic foot

V average free-stream air velocity, feet per second

M effective Mach number over span of model

M_a average chordwise Mach number

M_l local Mach number

R Reynolds number of wing, based on $\bar{c}$

α angle of attack, degrees

δ aileron deflection relative to wing-chord plane, measured perpendicular to aileron hinge axis (right wing panel; positive when trailing edge is down), degrees

L rolling moment, resulting from aileron deflection, about plane of symmetry, foot-pounds

N yawing moment, resulting from aileron deflection, referred to $0.25\bar{c}$ at plane of symmetry, foot-pounds

A wing aspect ratio $\left(\frac{b^2}{S}\right)$; for basic wing, 2.87, and for wing with extended tip, 4.83

$(C_D)_{C_L = 0}$ drag coefficient at zero lift

$C_{L_\alpha} = \left(\frac{\partial C_L}{\partial \alpha}\right)_\delta$

$C_{L_\delta} = \left(\frac{\partial C_L}{\partial \delta}\right)_\alpha$

$$C_{m_\delta} = \left(\frac{\partial C_m}{\partial \delta}\right)_\alpha$$

$$C_{l_\delta} = \left(\frac{\partial C_l}{\partial \delta}\right)_\alpha$$

The subscript outside the parentheses indicates the factor held constant during the measurement of the parameters in the vicinity of $\alpha = 0^\circ$ or $\delta = 0^\circ$.

MODEL AND APPARATUS

The basic semispan wing had 51.3° of sweepback at the leading edge, a taper ratio of 0.51, an aspect ratio of 2.87, a thickness-chord ratio of 8.3 percent, and an NACA 64_1-012 airfoil section perpendicular to the 0.556-chord line. A drawing of the basic-wing model mounted on the transonic bump is shown in figure 1. The semispan wing with extended-tip plan form was obtained by extending the leading edge to intersect a line perpendicular to the tip-chord line at the trailing edge of the tip chord. A sketch of the model with extended tip is shown in figure 2. The extended-tip wing had 51.3° sweepback at the leading edge, an aspect ratio of 4.83, and an NACA 64_1-012 airfoil section perpendicular to the 0.556-chord line. The extended-tip section was generated by straight line elements from the tip to the airfoil section at the tip of the basic wing. The basic wing was made of beryllium-copper and bismuth-tin alloys, while the extended tips were made of brass.

Three ailerons were used during the present investigation, one with the basic-wing plan form and two with the extended-tip-wing plan form. The aileron used on the basic wing was triangular in plan form and was deflected about a hinge axis perpendicular to the leading edge of the wing (fig. 1). One aileron used with the extended-tip-wing plan form was obtained by deflecting the triangular extended tip area about a spanwise axis through the 0.50-tip-chord station of the basic wing (fig. 2(a)), while the other was obtained by deflecting the area of the wing aft of a spanwise axis through the 0.50-tip-chord station of the basic wing (fig. 2(b)).

The model was mounted vertically on an electrical strain-gage balance enclosed within the bump, and the wing lift, drag, pitching moment, yawing moment, and rolling moment were recorded by calibrated electrical potentiometers. The balance chamber was sealed except for a rectangular clearance hole through which the model butt extension passed. This hole was sealed by a sponge-rubber seal mounted on the under surface of the bump turntable.

TEST TECHNIQUE

The tests were made in the Langley high-speed 7- by 10-foot tunnel by means of the transonic-bump technique; that is, the model was tested in the local high-speed region obtained over the curved surface of a bump mounted on the floor of the tunnel (reference 5).

Typical contours showing the Mach number distribution over the bump in the vicinity of the model are presented in figure 3. The effective test Mach number was obtained from contour charts similar to figure 3 by use of the relationship

$$M = \frac{2}{S} \int_0^{b/2} cM_a \, dy$$

It may be noted that the ailerons, being at the wing tip, were located in a region where the local Mach number was as much as 0.05 lower than the effective test Mach number. No attempt was made to evaluate the effect of this Mach number variation on the data.

Force and moment data were obtained through a Mach number range of 0.60 to 1.15 and an angle-of-attack range of -16° to 16°. The ailerons were investigated through a deflection range of 0° to 45°. The variation of average Reynolds number with Mach number for the two model spans investigated is presented in figure 4.

CORRECTIONS

The lift and pitching moments represent data for the complete wing with controls mounted on both semispans. The drag, rolling moments, and yawing moments presented herein represent the incremental effects on the complete wing produced by the deflection of the control on only one semispan of the complete wing. No reflection-plane corrections were applied to the data, since no corrections are available for this type of control configuration; however, corrections as applied to conventional wing-aileron configurations at low speed indicate that the rolling-moment coefficients would not be reduced by more than 10 percent.

DISCUSSION

The longitudinal aerodynamic characteristics of the basic wing and the wing with extended tip are presented in figure 5 for three representative Mach numbers and are summarized in figure 6. The angle of attack and pitching-moment coefficient plotted against lift coefficient were generally linear from $C_L = -0.2$ to $C_L = 2$, and slopes were taken within this range. The data show that the wing with extended tip has a slightly higher lift-curve slope C_{L_α}, which can be attributed to the increased aspect ratio and improved flow of the wing with extended tip. Asymmetry of the drag data, figure 5, can be attributed to inaccuracies of model construction and to cross flow over the bump. It may be noted that the drag at zero lift would be slightly lower if the drag data were entirely symmetric. The pitching-moment data of the basic wing indicate that the wing was stable at low lift coefficients (between $C_L = -0.4$ and $C_L = 0.4$) with an unstable break at lift coefficients above $C_L = 0.5$. The wing with extended tip was stable at low lift coefficients but had an unstable break at about $C_L = 0.4$.

There was little change in lift-curve slope as the Mach number was increased (fig. 6). The data indicated a sharp increase in drag at $C_L = 0$ between $M = 0.95$ and $M = 1.00$. The aerodynamic center of the basic wing was about $0.27\bar{c}$ up to $M = 1.00$ and increased to $0.38\bar{c}$ at $M = 1.15$; for the wing with extended tip the aerodynamic center was $0.36\bar{c}$ at $M = 0.60$, decreased to $0.30\bar{c}$ at $M = 1.00$, and increased to $0.43\bar{c}$ at $M = 1.15$ (fig. 6).

The aerodynamic characteristics plotted against control deflection for each Mach number investigated are presented in figure 7 for the triangular deflectable-tip aileron on the basic wing, figure 8 for the triangular deflectable-tip aileron on the wing with extended tip, and figure 9 for the trapezoidal trailing-edge aileron on the wing with extended tip.

The ailerons produced changes in lift and pitching moment throughout the Mach number range investigated except at high angles of attack, and these variations of lift and pitching moment with aileron deflection were generally linear at deflections up to $\delta = \pm 15^\circ$.

The values of incremental-drag coefficient at a specific aileron deflection generally increased with increase in Mach number up to $M = 1.05$ and decreased slightly from $M = 1.05$ to $M = 1.15$.

The rolling-moment data for the triangular aileron on the basic wing, figure 7, indicated that the aileron was generally effective in producing roll at Mach numbers below $M = 0.90$, but experienced a large reduction in effectiveness between $M = 0.90$ and $M = 1.03$. The aileron was again effective above $M = 1.03$ (fig. 10).

The rolling-moment data for the triangular aileron on the wing with the extended tip, figure 8, indicate that a reduction in rolling moment occurred for positive aileron deflections at positive angles of attack. As the Mach number was increased, this reduction in rolling moment became more apparent, particularly at Mach numbers above $M = 1.00$. Similar effects of reduction of aileron effectiveness at high positive values of α and δ were exhibited by the low-speed data of reference 2 and can possibly be attributed to tip stall or interference effects between the deflected tip and the wing. The data of figure 9 for the wing with the extended tip with the parallelogram aileron showed that the aileron was effective in producing roll for aileron deflections up to $\delta = \pm 15^{\circ}$ at all angles of attack throughout the Mach number range investigated. A reduction in rolling effectiveness occurred at higher positive or negative aileron deflections.

Assuming equal aileron deflections, the yawing-moment data for the various aileron configurations investigated (figs. 7 to 9) were generally adverse throughout the Mach number range investigated and became more adverse with increase in angle of attack and aileron deflection. At higher deflections, the adverse C_n/C_l ratio was as high as 0.6 for all ailerons investigated.

The control-effectiveness parameters presented against Mach number for the three ailerons investigated were obtained from figures 7 to 9 and are shown in figure 10. The aerodynamic characteristics of the three ailerons investigated were generally linear from $\delta = 15^{\circ}$ to $\delta = -15^{\circ}$ and the slopes presented were obtained within this range at $\alpha = 0^{\circ}$.

Lift effectiveness $C_{L_{\delta}}$ and pitching-moment effectiveness $C_{m_{\delta}}$ for the triangular aileron on the basic wing were almost constant up to high-subsonic speeds ($M = 0.90$) and decreased sharply to $M = 1.00$; for the triangular aileron on the wing with extended tip, $C_{L_{\delta}}$ increased up to $M = 1.00$ and decreased above $M = 1.00$, and $C_{m_{\delta}}$ was almost constant up to $M = 1.00$ and increased sharply at $M = 1.00$. The parameters $C_{L_{\delta}}$ and $C_{m_{\delta}}$ for the trapezoidal aileron were almost constant throughout the Mach number range.

The rolling-moment parameter $C_{l_{\delta}}$ for each aileron was generally constant with increase in Mach number except for a large loss in effectiveness in the transonic speed range for the triangular aileron on the basic wing.

The trapezoidal aileron on the wing with extended tip gave the most favorable $C_{L_{\delta}}$, $C_{m_{\delta}}$, and $C_{l_{\delta}}$ and the values changed only slightly with increase in Mach number.

CONCLUSIONS

An investigation through the transonic speed range of three wing-tip ailerons, on a 51.3° sweptback semispan wing, was made in the Langley high-speed 7- by 10-foot tunnel. The results of the investigation indicate the following conclusions:

1. The triangular wing-tip aileron tested on the basic wing provided lateral control at Mach numbers up to 0.90, but experienced a large loss in control effectiveness between Mach numbers of 0.90 and 1.03.

2. The triangular and trapezoidal wing-tip ailerons tested on the extended-tip wing provided lateral control over the entire Mach number range, except at very high angles of attack, where the rolling effectiveness was appreciably reduced.

3. Assuming equal aileron deflections the yawing moments resulting from aileron deflection for all wing-tip ailerons investigated were generally adverse throughout the Mach number range investigated.

Langley Aeronautical Laboratory
National Advisory Committee for Aeronautics
Langley Field, Va.

REFERENCES

1. Lowry, John G., and Schneiter, Leslie E.: Investigation at Low Speed of the Longitudinal Stability Characteristics of a 60° Swept-Back Tapered Low-Drag Wing. NACA TN 1284, 1947.

2. Hagerman, John R., and O'Hare, William M.: Investigation of Extensible Wing-Tip Ailerons on an Untapered Semispan Wing at 0° and 45° Sweepback. NACA RM L9H04, 1949.

3. Fischel, Jack, and Watson, James M.: Low-Speed Investigation of Deflectable Wing-Tip Ailerons on an Untapered 45° Sweptback Semi-Span Wing with and without an End Plate. NACA RM L9J28, 1949.

4. Turner, Thomas R., Lockwood, Vernard E., and Vogler, Raymond D.: Preliminary Investigation of Various Ailerons on a 42° Sweptback Wing for Lateral Control at Transonic Speeds. NACA RM L8D21, 1948.

5. Schneiter, Leslie E., and Ziff, Howard L.: Preliminary Investigation of Spoiler Lateral Control on a 42° Sweptback Wing at Transonic Speeds. NACA RM L7F19, 1947.

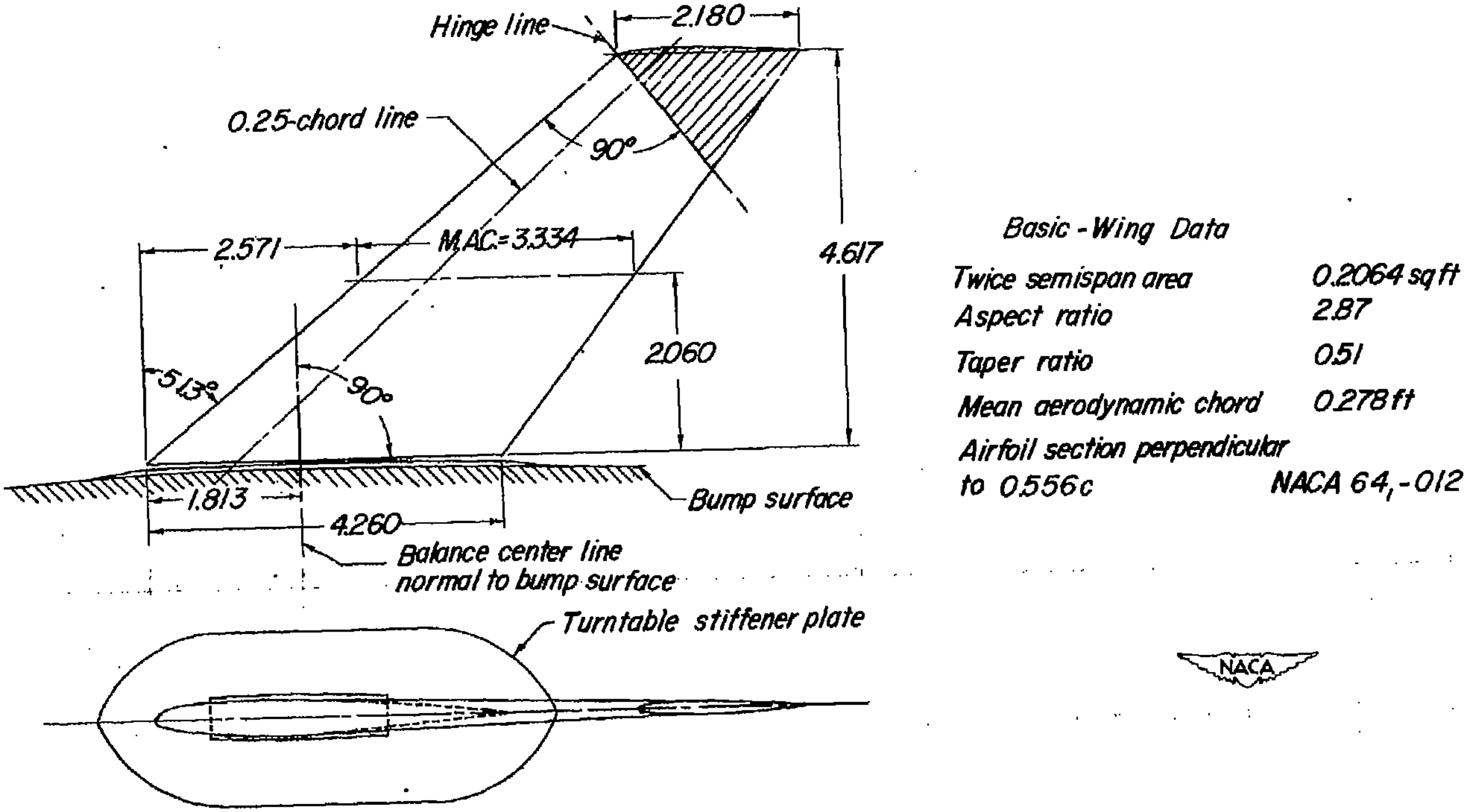

Figure 1.- General arrangement of the 51.3° sweptback wing with triangular deflectable-tip aileron. (All dimensions are in inches.)

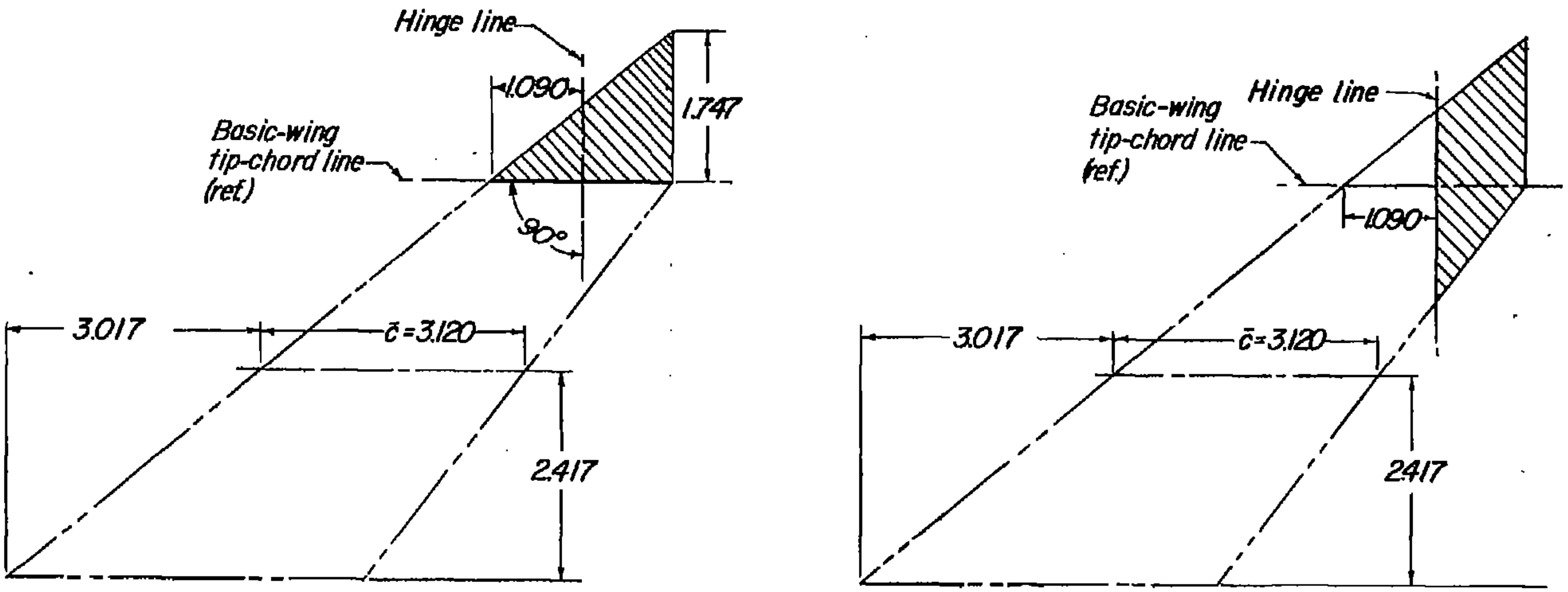

(a) Triangular aileron

(b) Trapezoidal aileron

Extended-Tip-Wing Data

Twice semispan area	0.2328 sq ft
Aspect ratio	4.83
Mean aerodynamic chord	0.260 ft
Airfoil section perpendicular to 0.556c	NACA 64_1-012

Figure 2.- General arrangement of the 51.3° sweptback wing with extended tip with triangular and trapezoidal ailerons. (All dimensions are in inches.)

CONFIDENTIAL

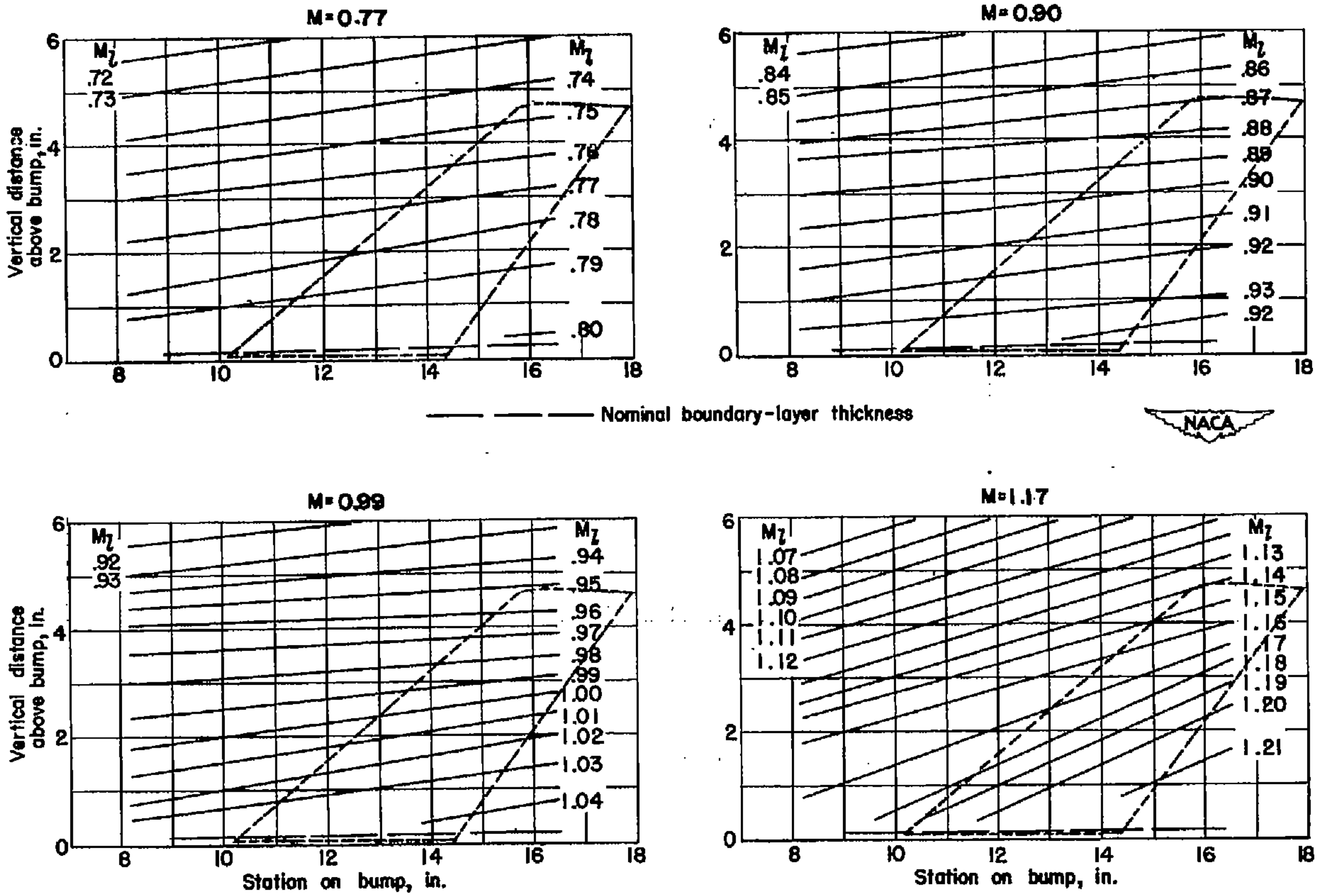

Figure 3.- Typical Mach number contours over transonic bump in region of model location.

CONFIDENTIAL
SECURITY INFORMATION

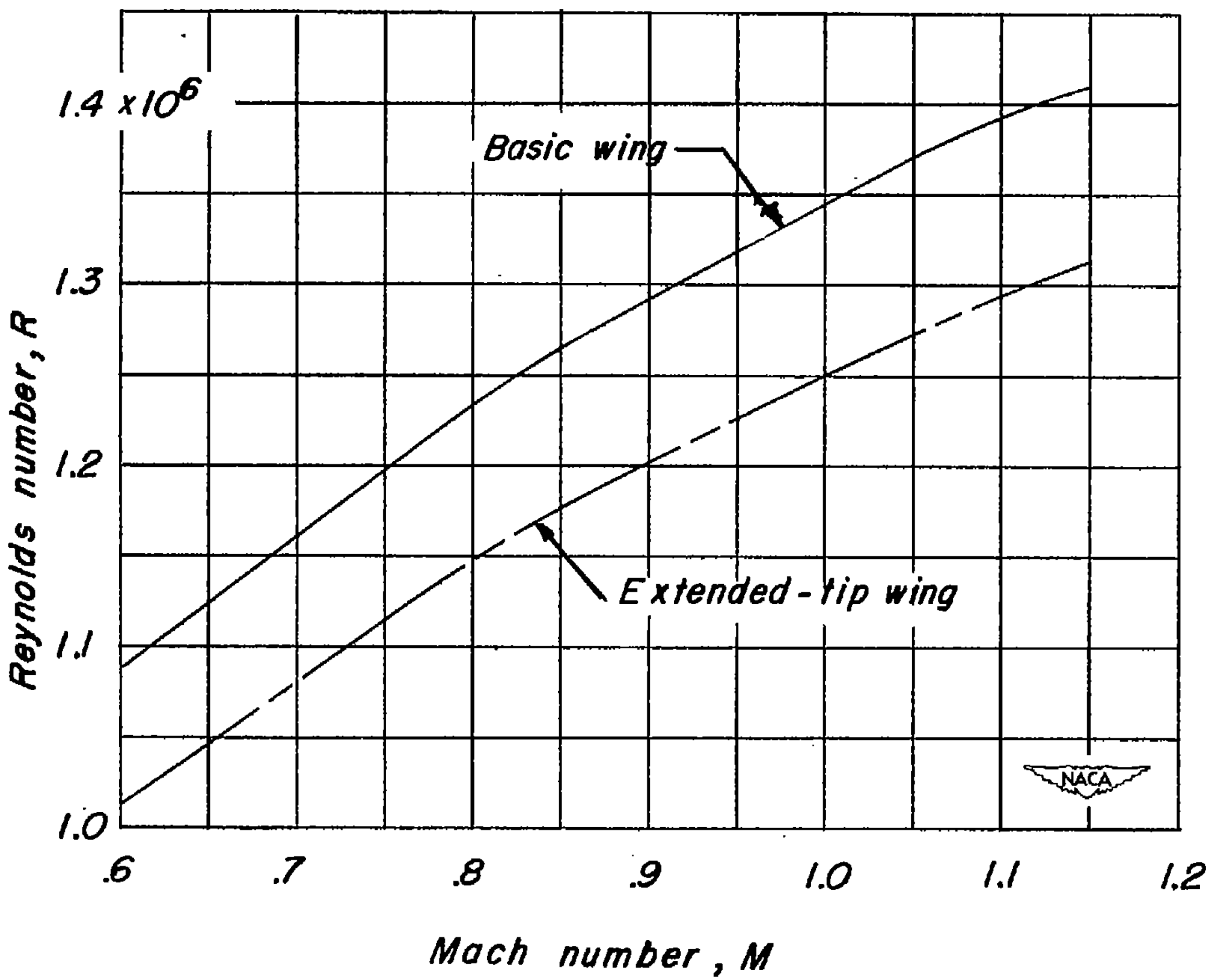

Figure 4.- Variation of test Reynolds number with Mach number for the basic wing model and the model with extended tip.

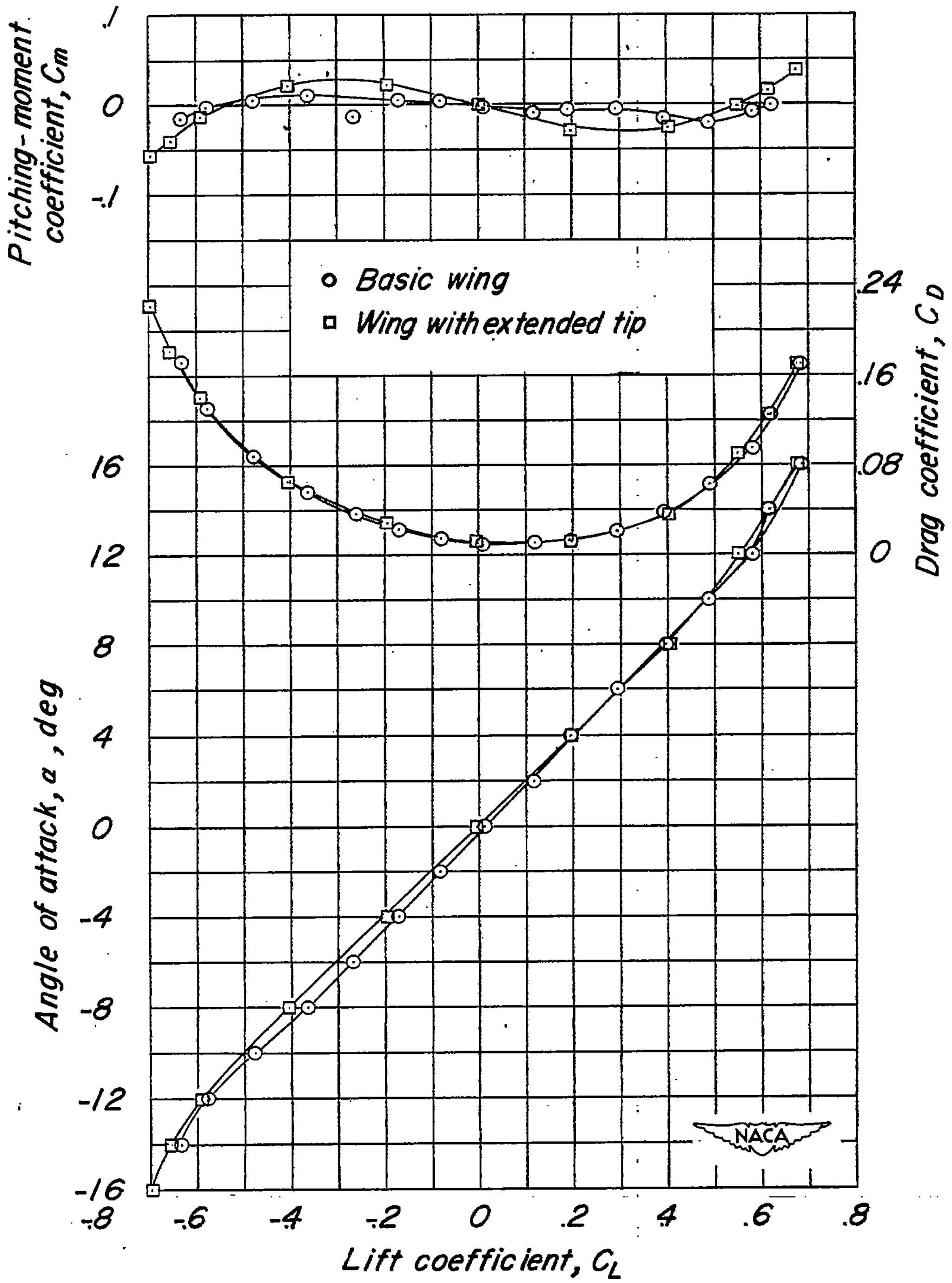

(a) M = 0.60.

Figure 5.- The aerodynamic characteristics in pitching of the 51.3° sweptback wing with and without extended tip.

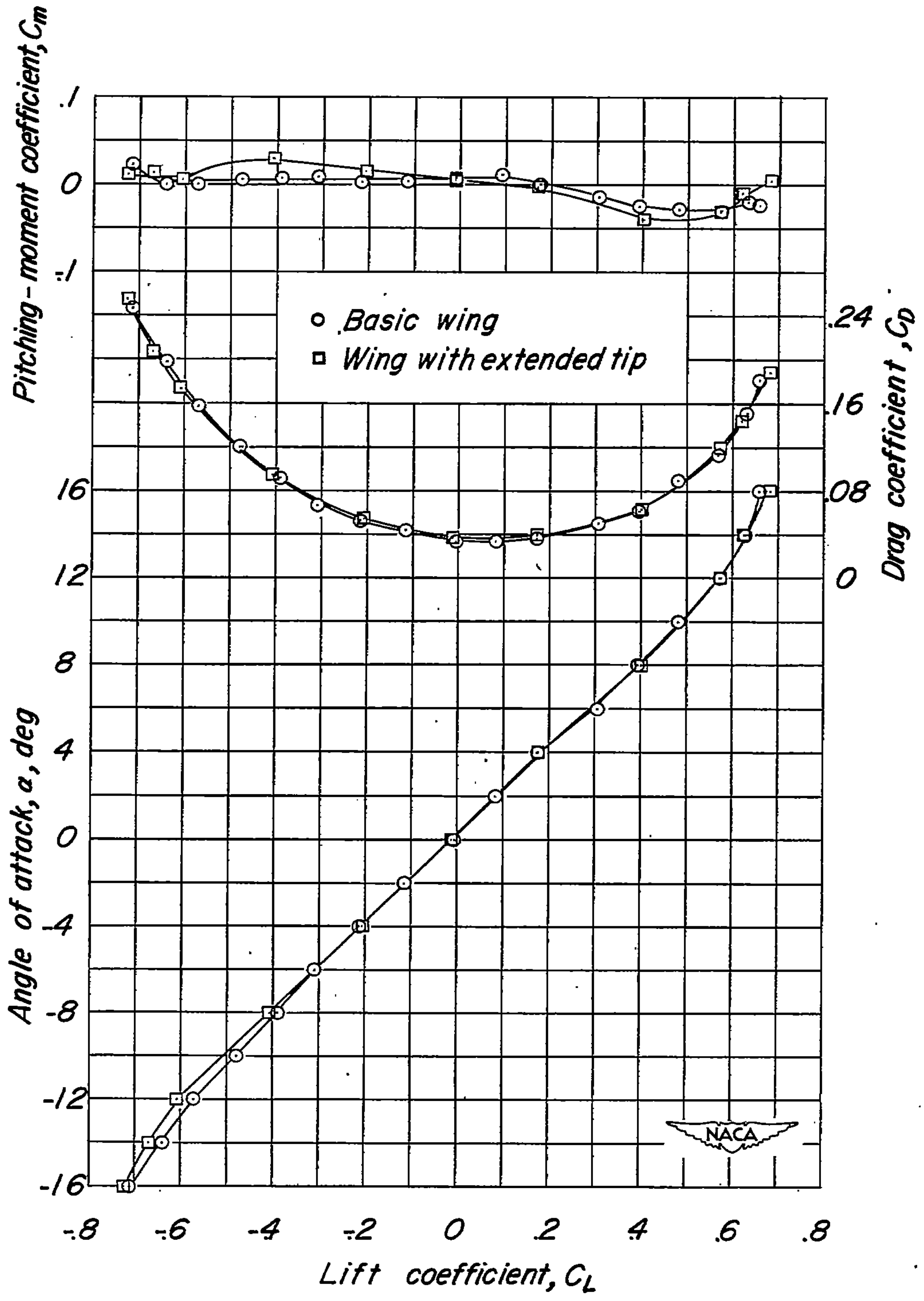

(b) M = 1.00.

Figure 5.- Continued.

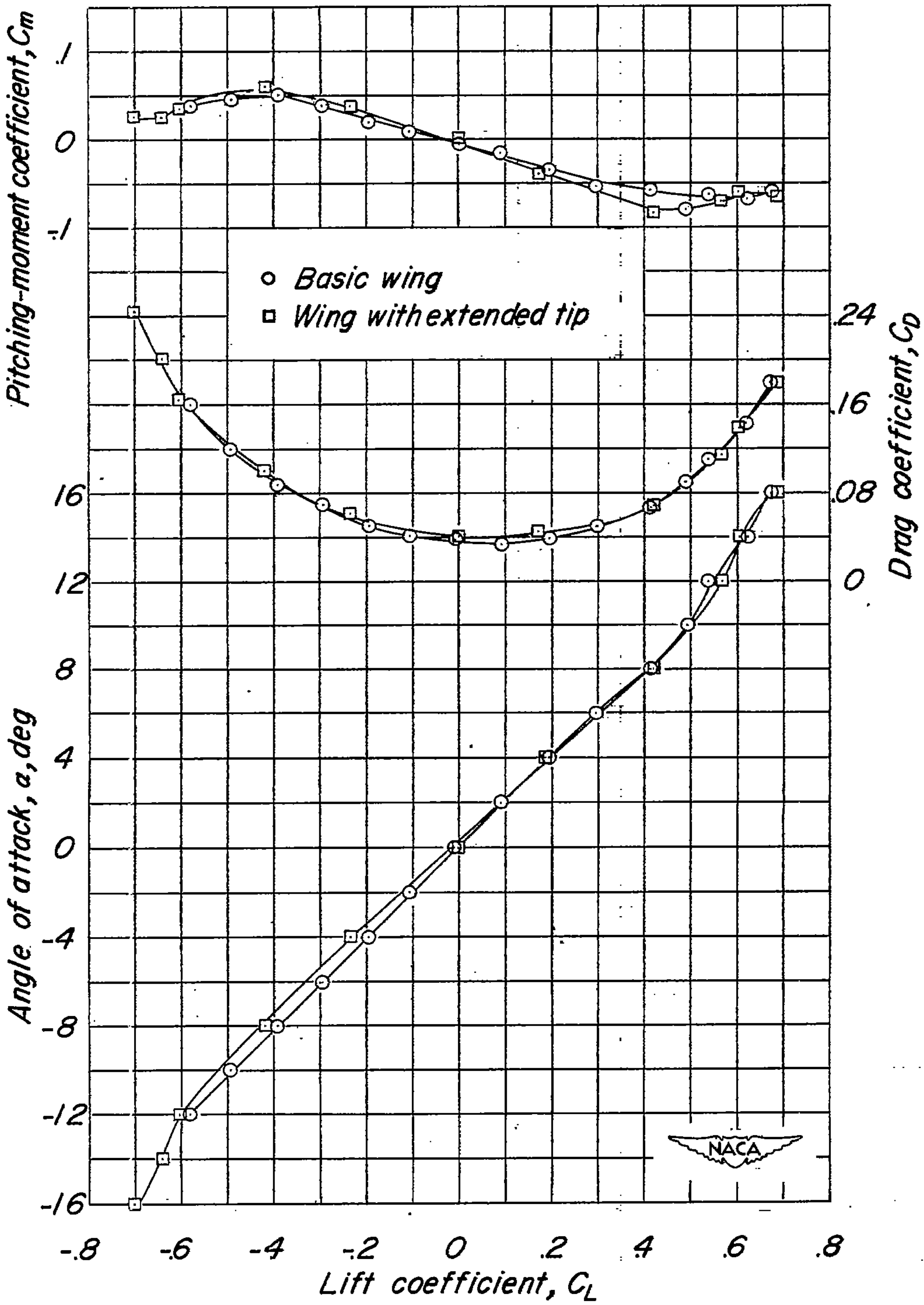

(c) M = 1.15.

Figure 5.- Concluded.

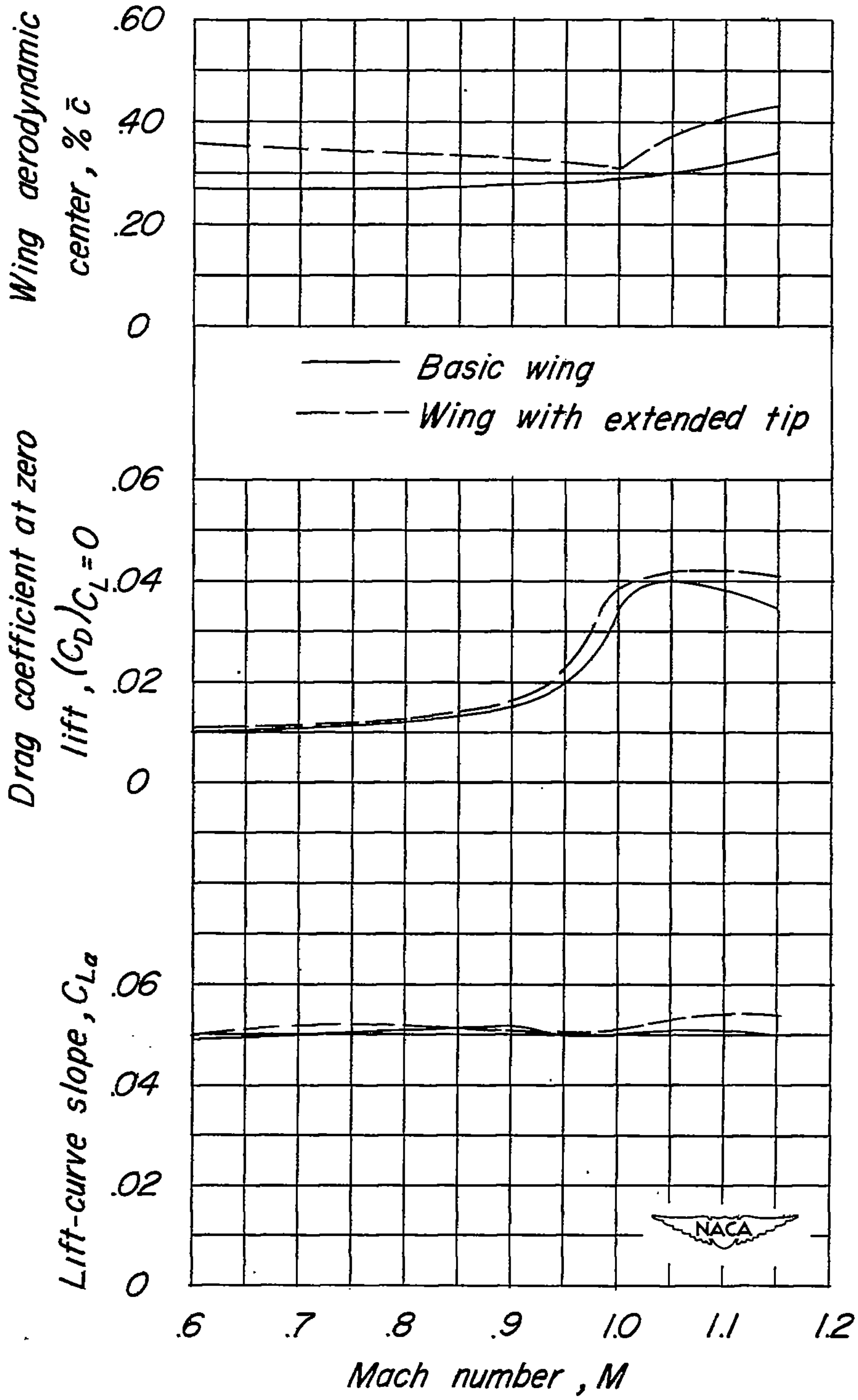

Figure 6.- The variation of lift-curve slope, drag coefficient at $C_L = 0$, and aerodynamic center with Mach number for the basic wing and the wing with extended tip.

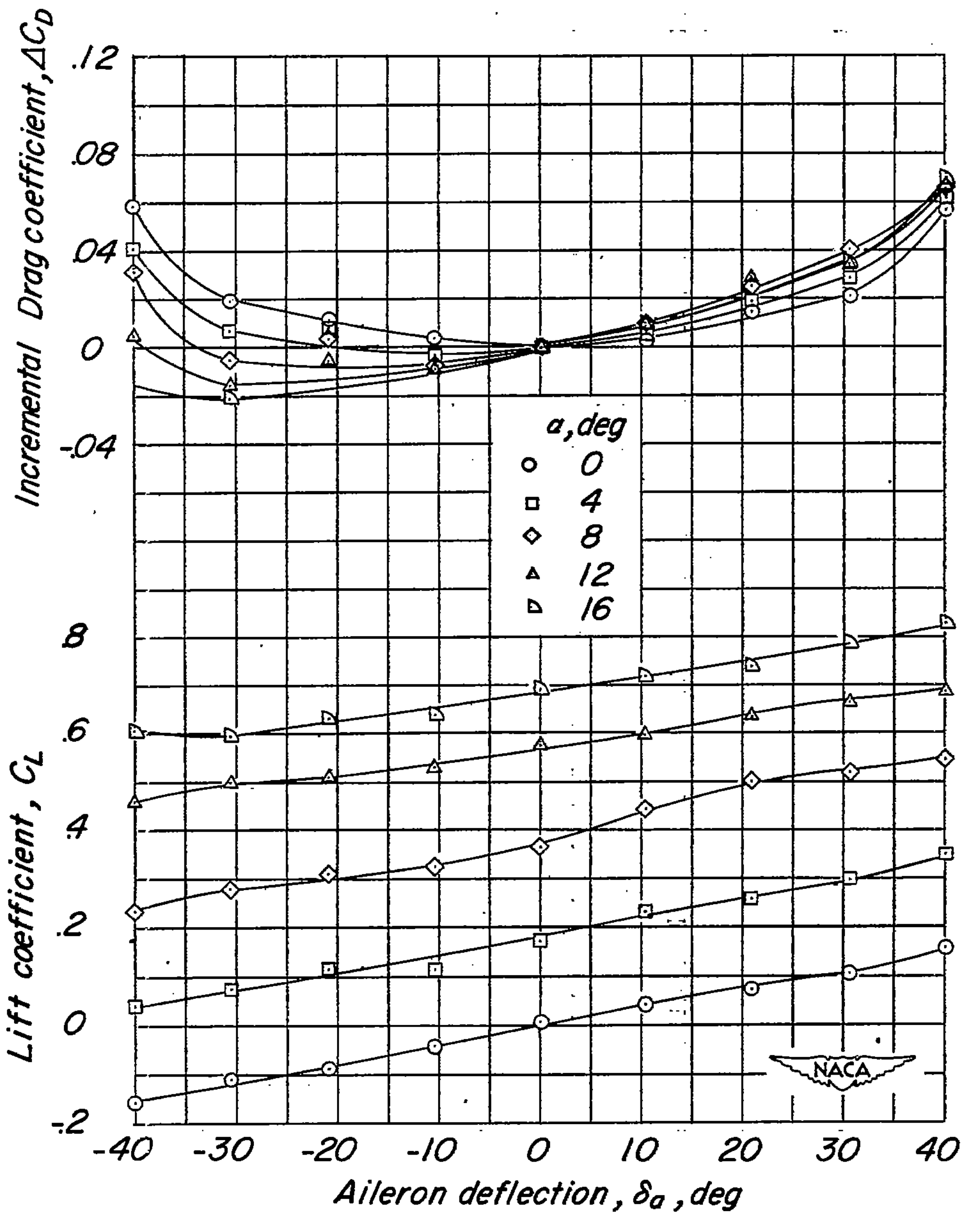

(a) M = 0.60.

Figure 7.- Aerodynamic characteristics of 51.3° sweptback wing with triangular deflectable-tip aileron; aspect ratio 2.67 and taper ratio 0.51.

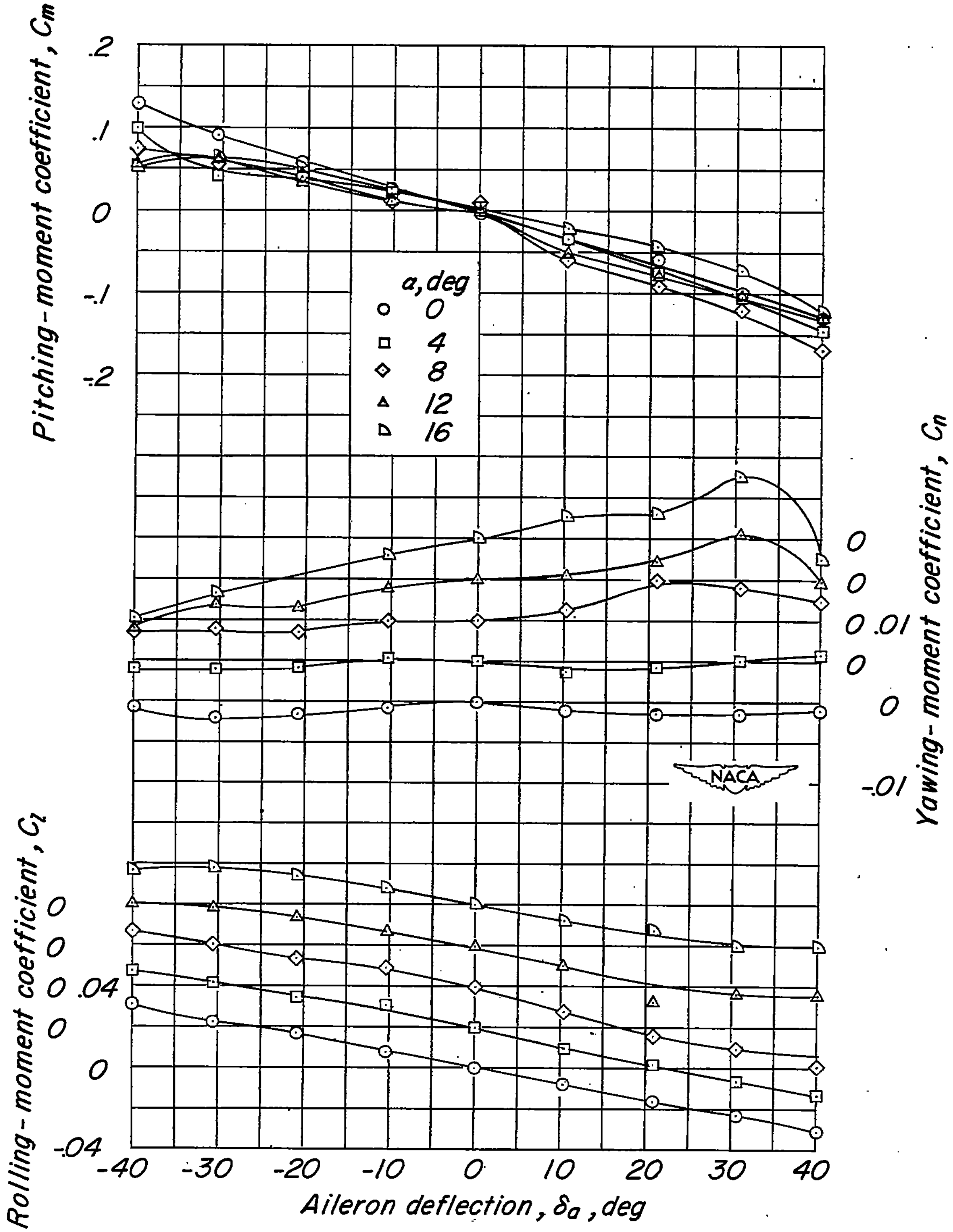

(a) Concluded.

Figure 7.- Continued.

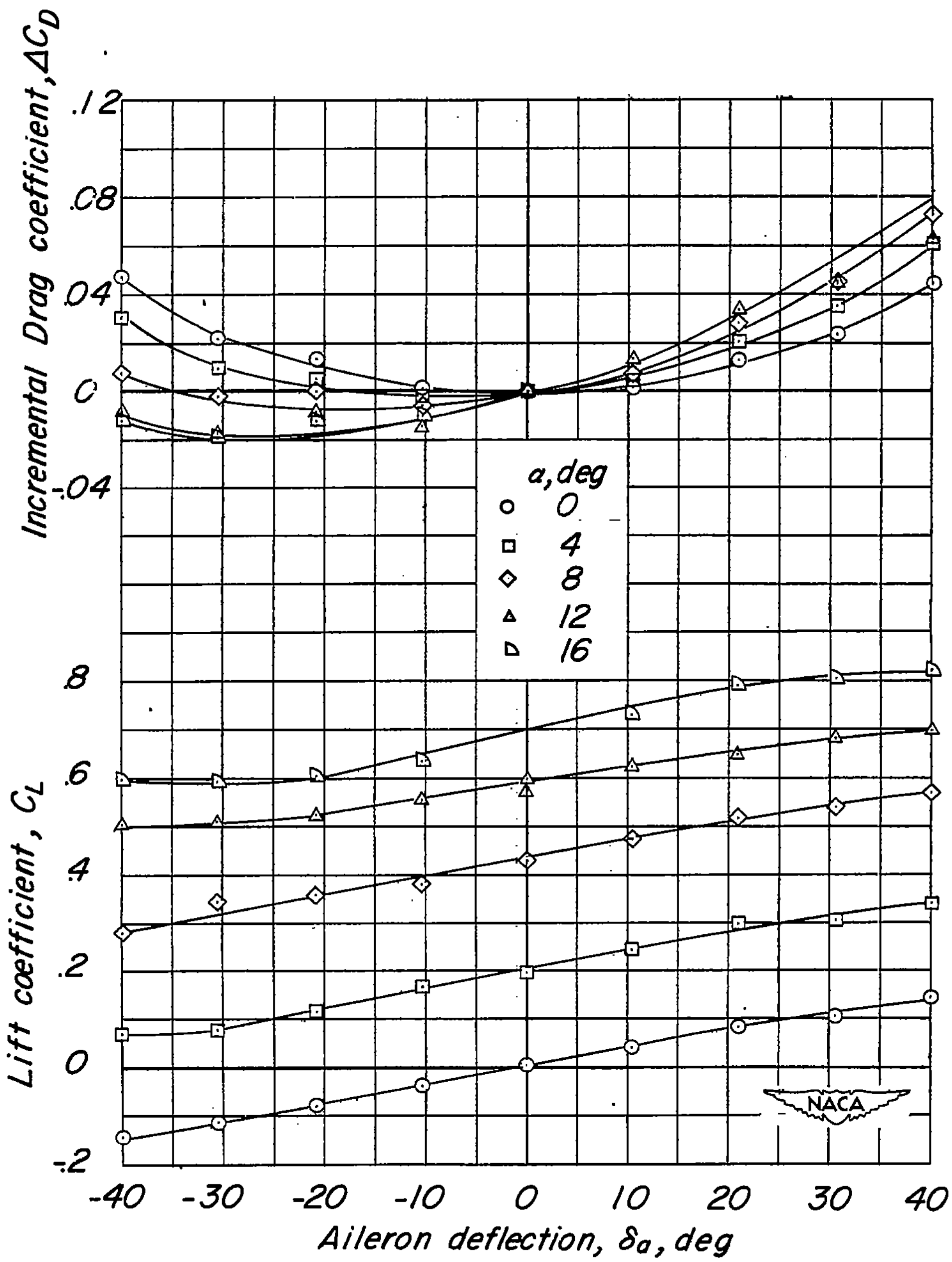

(b) M = 0.80.

Figure 7.- Continued.

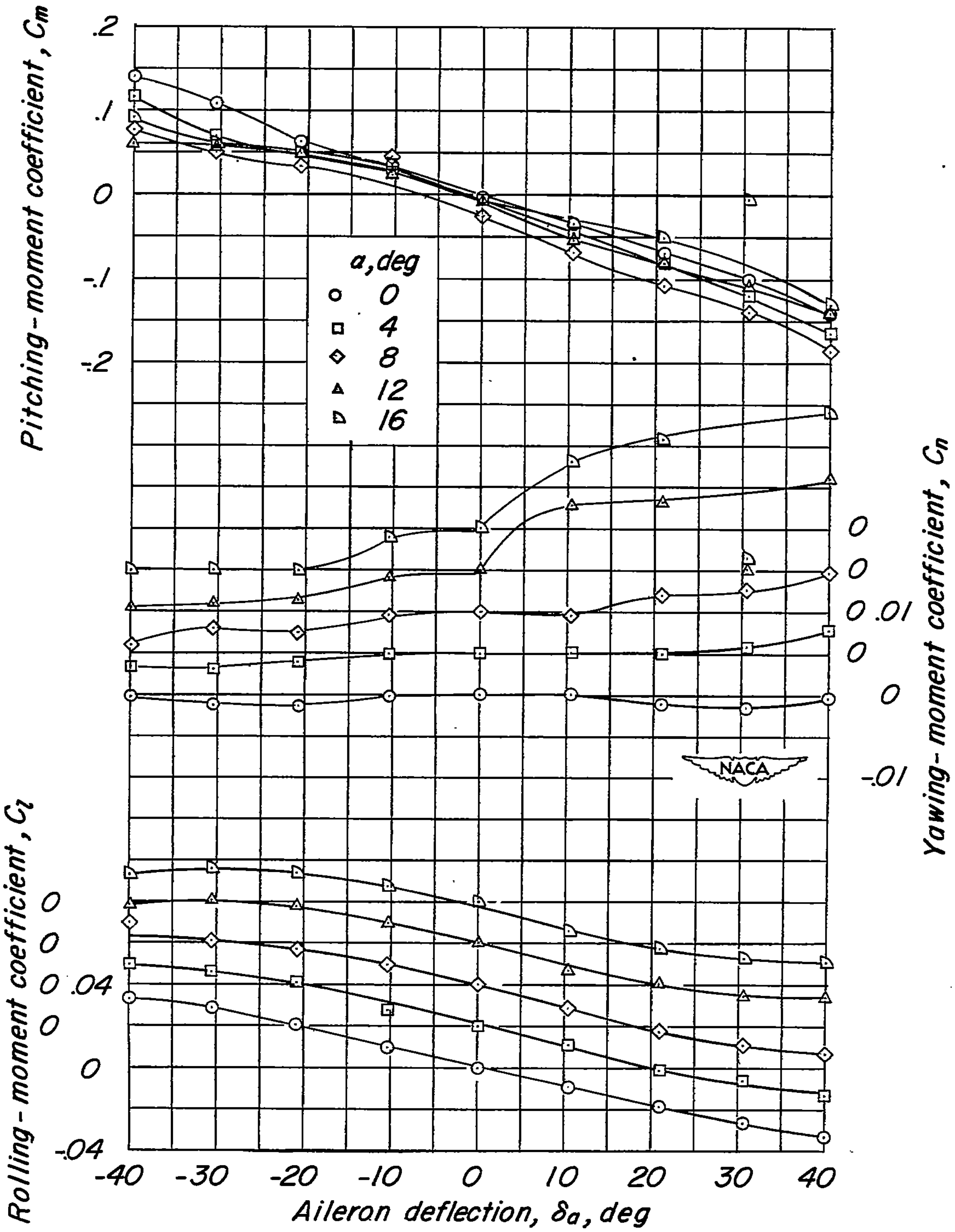

(b) Concluded.

Figure 7.- Continued.

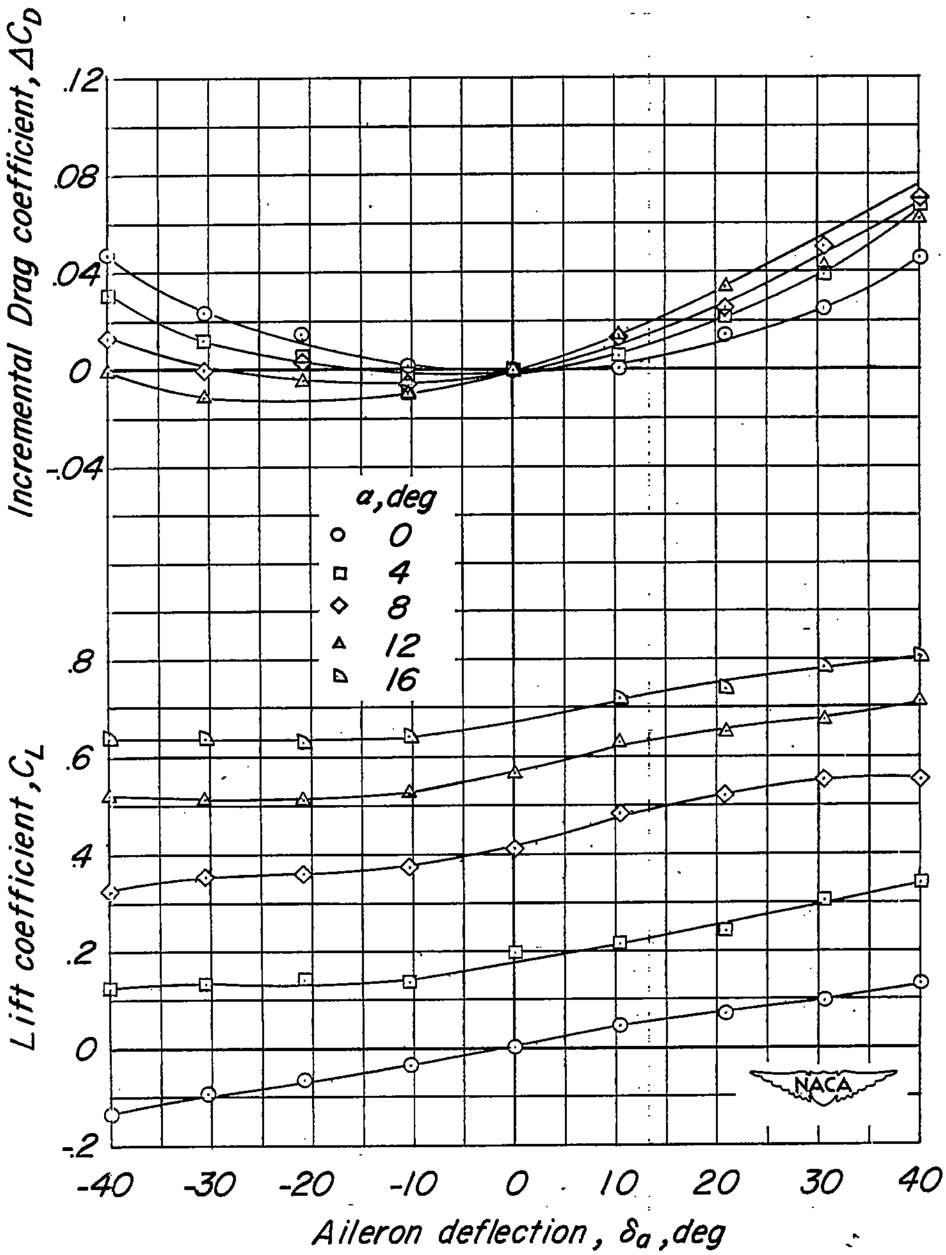

(c) M = 0.90.

Figure 7.- Continued.

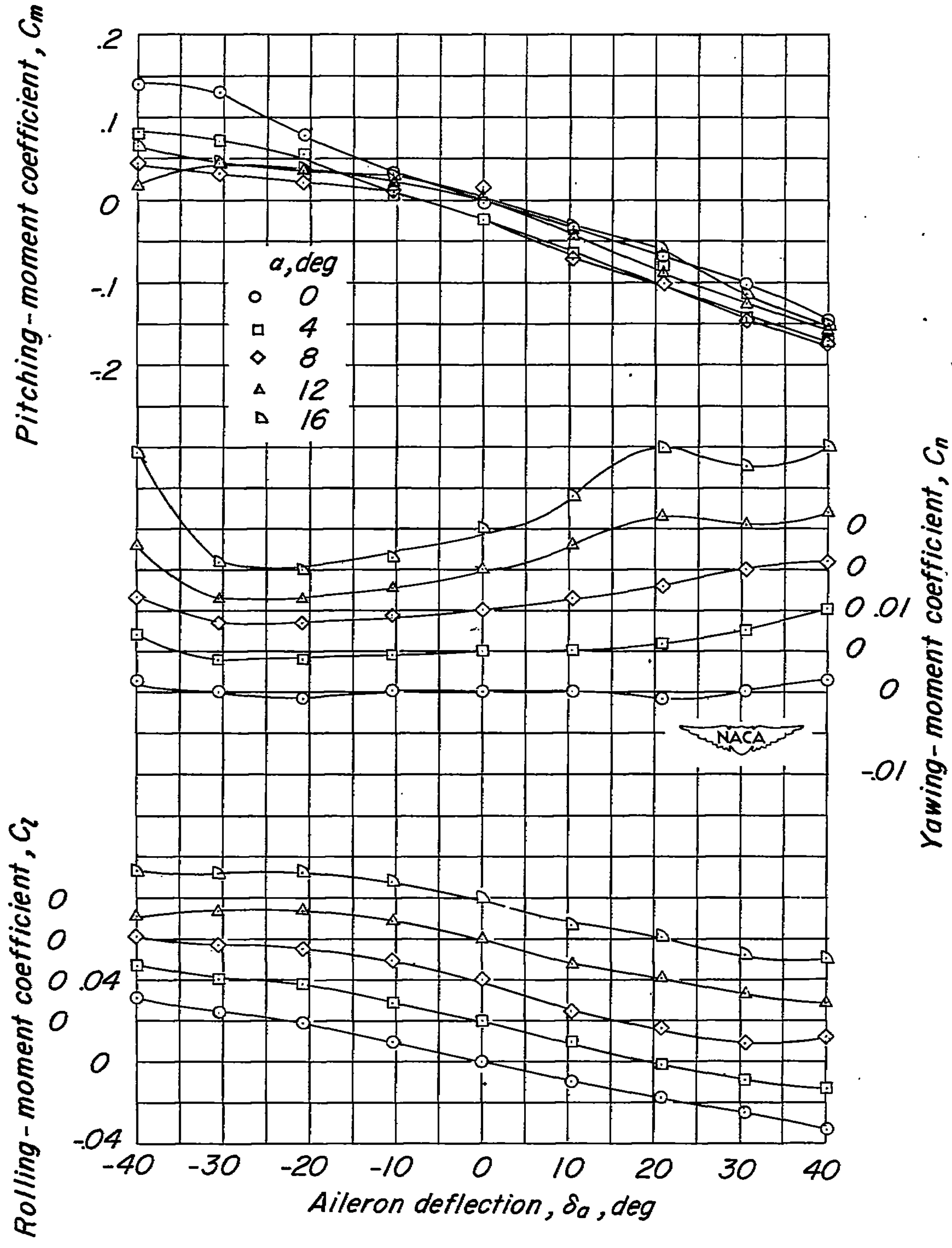

(c) Concluded.

Figure 7.- Continued.

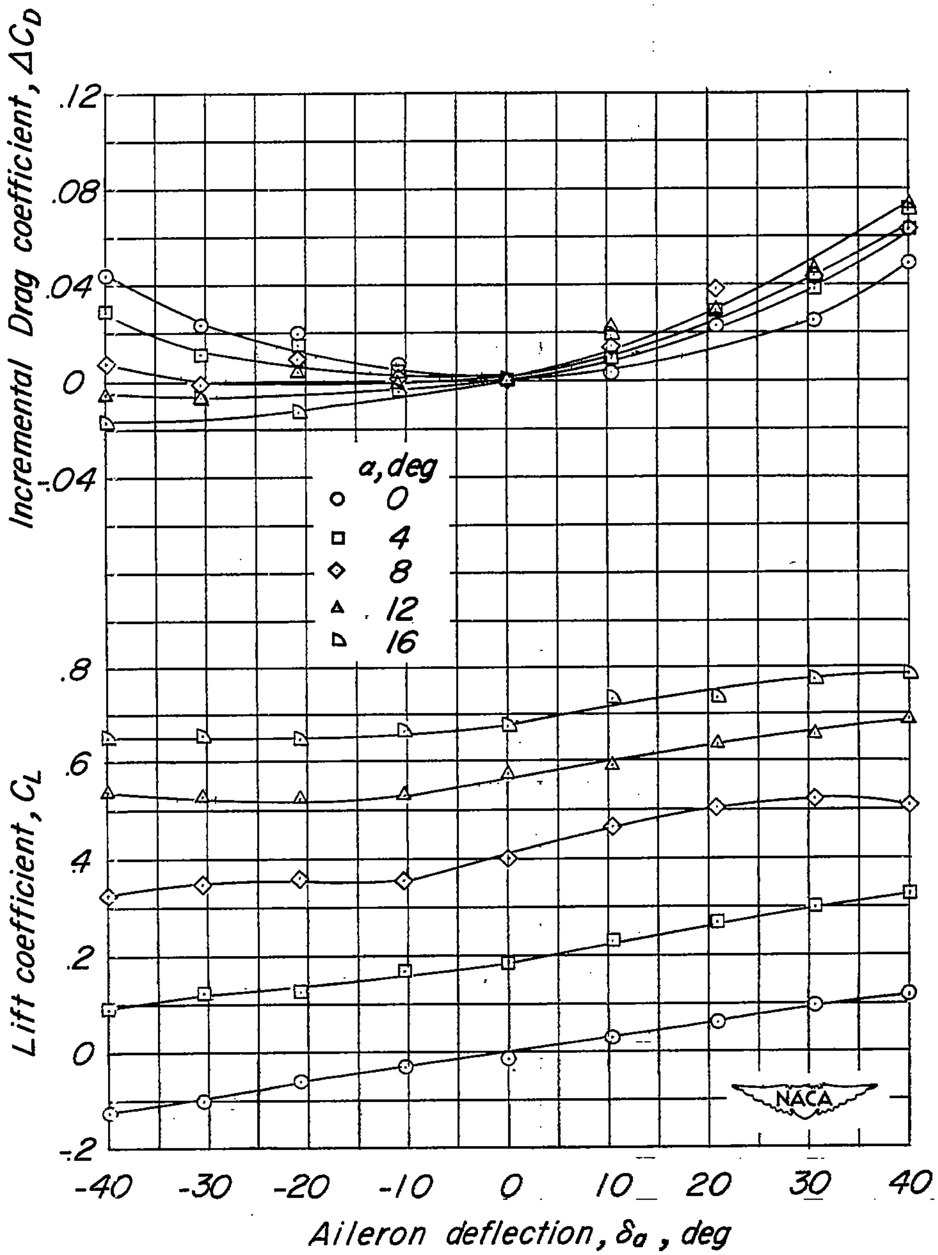

(d) M = 0.95.

Figure 7.- Continued.

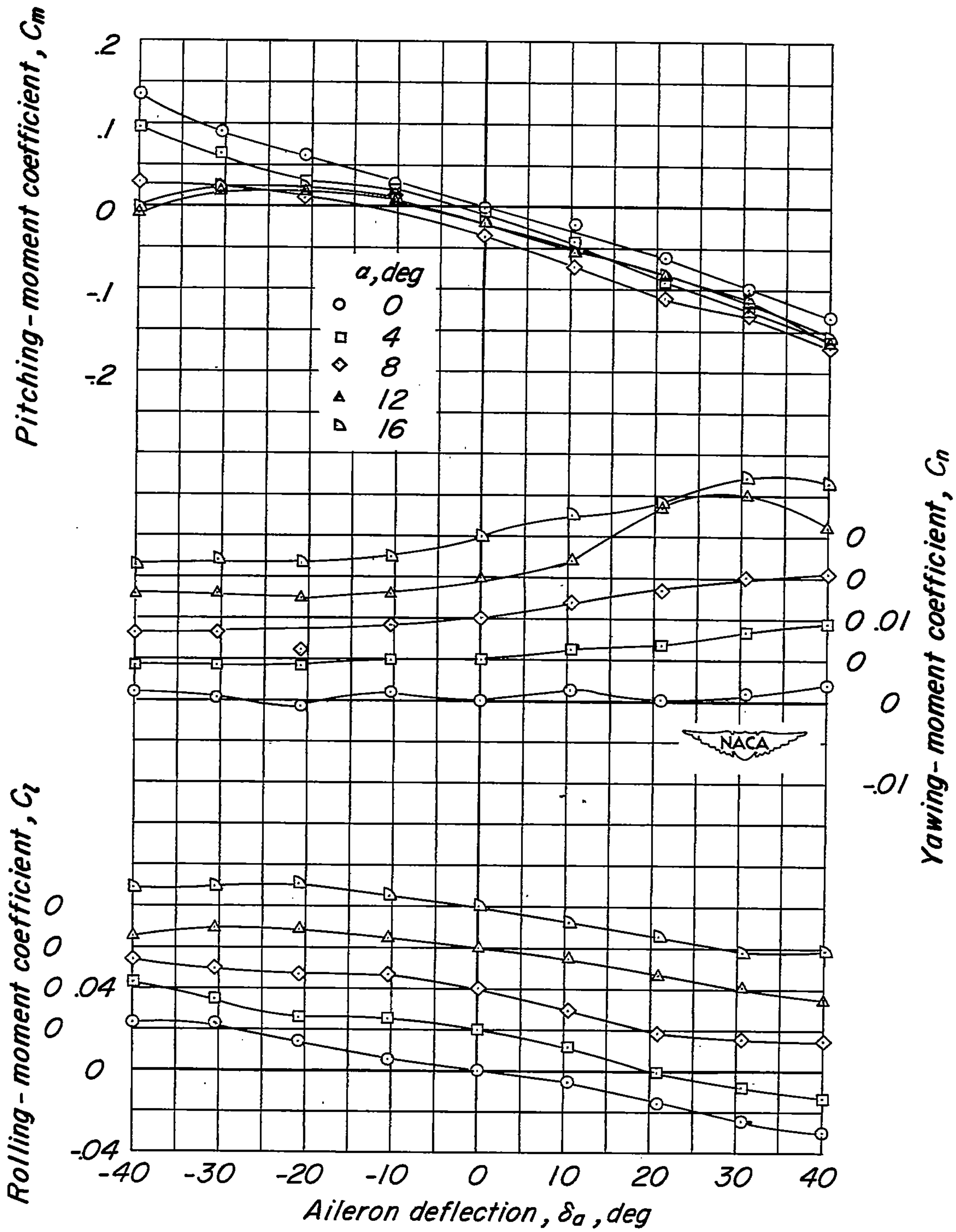

(d) Concluded.

Figure 7.- Continued.

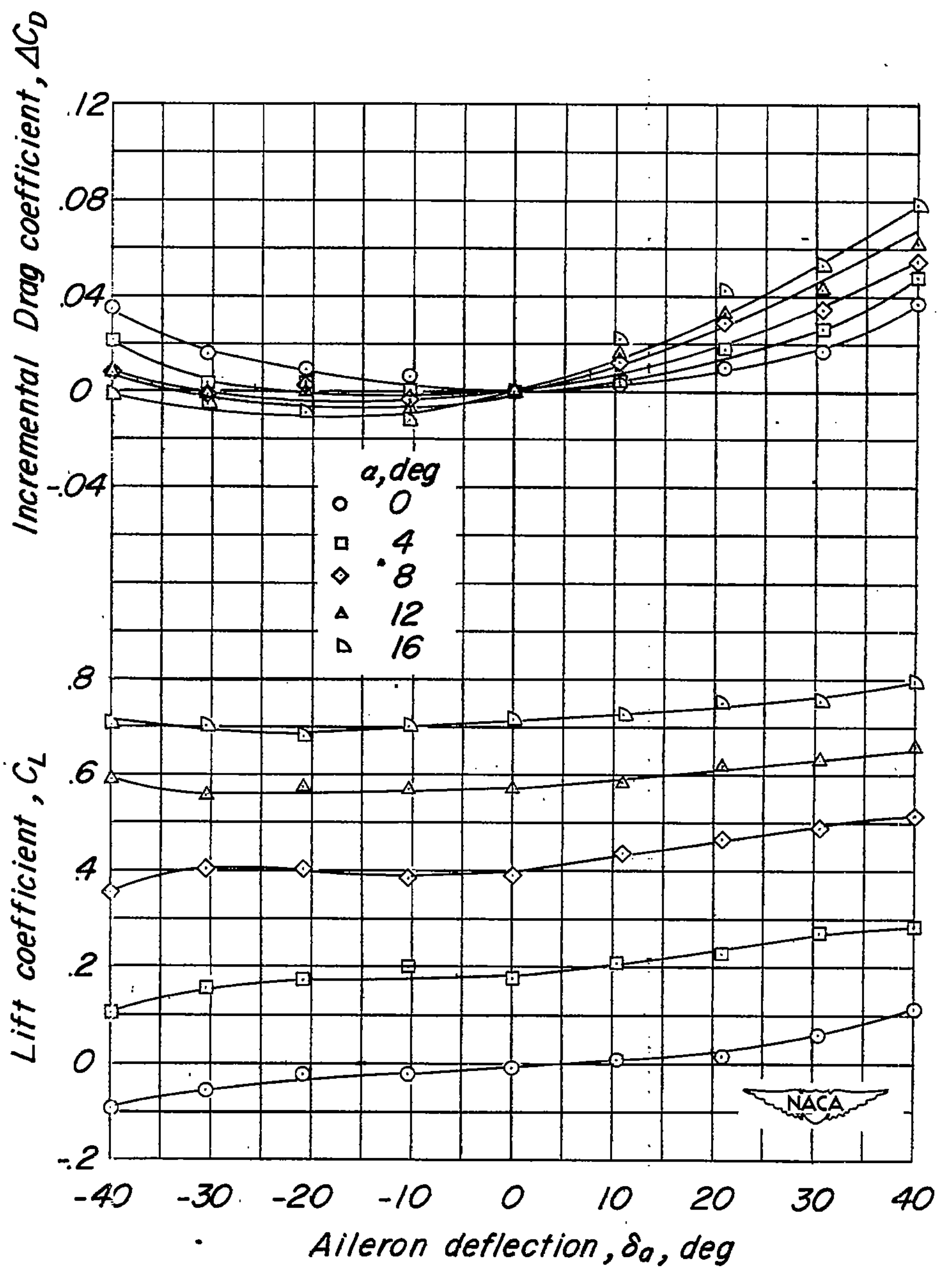

(e) M = 1.00.

Figure 7.- Continued.

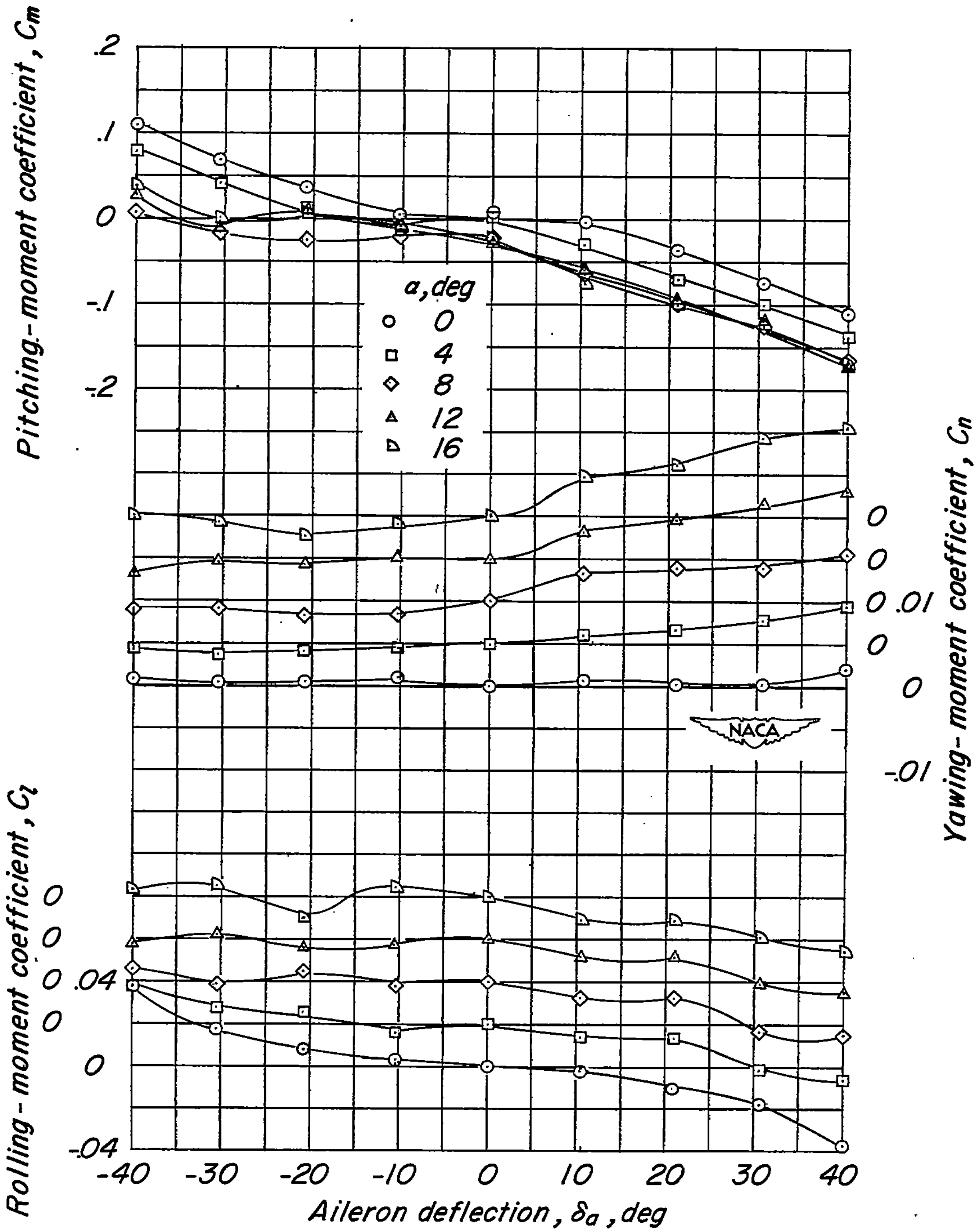

(e) Concluded.

Figure 7.- Continued.

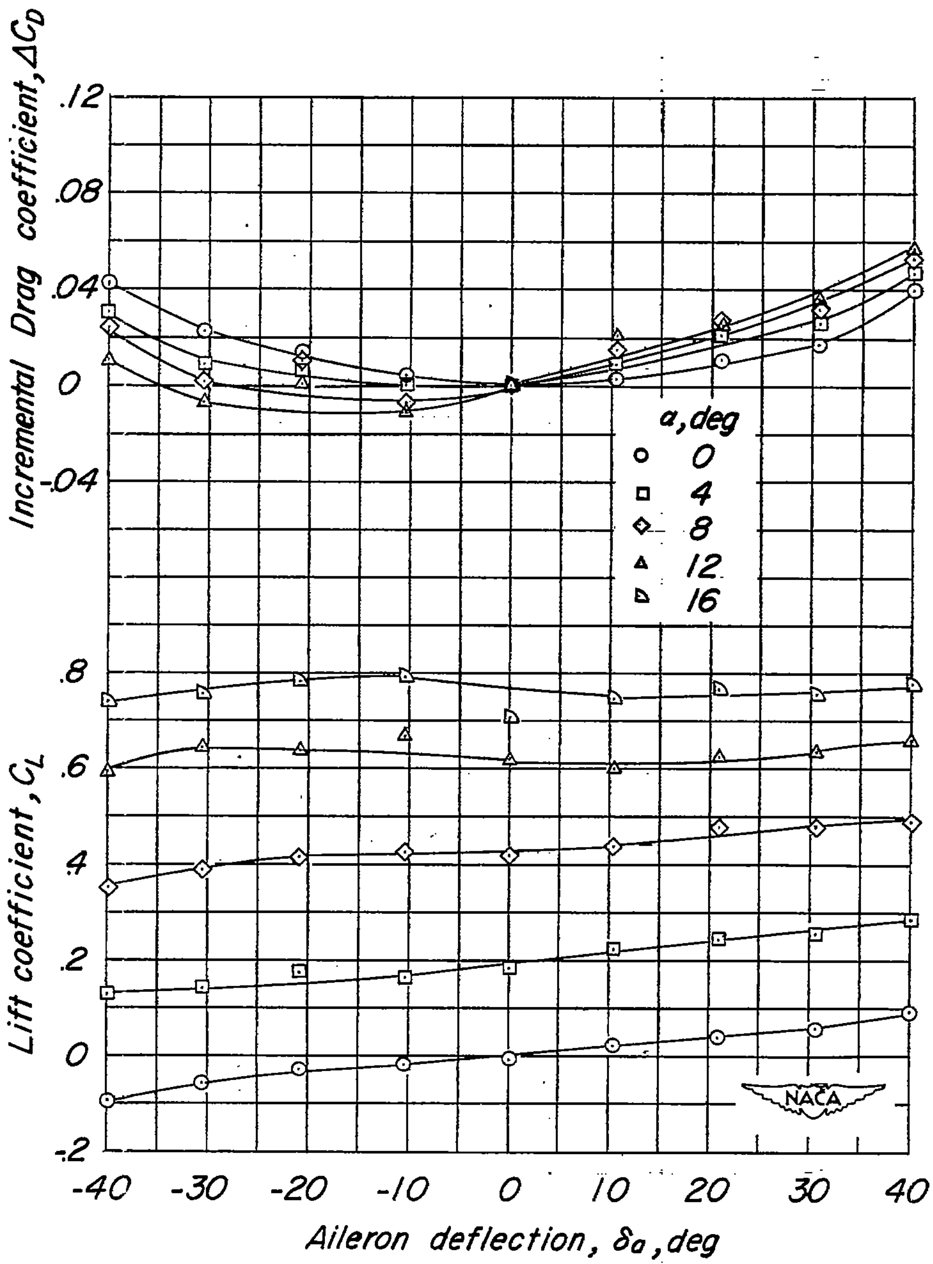

(f) M = 1.05.

Figure 7.- Continued.

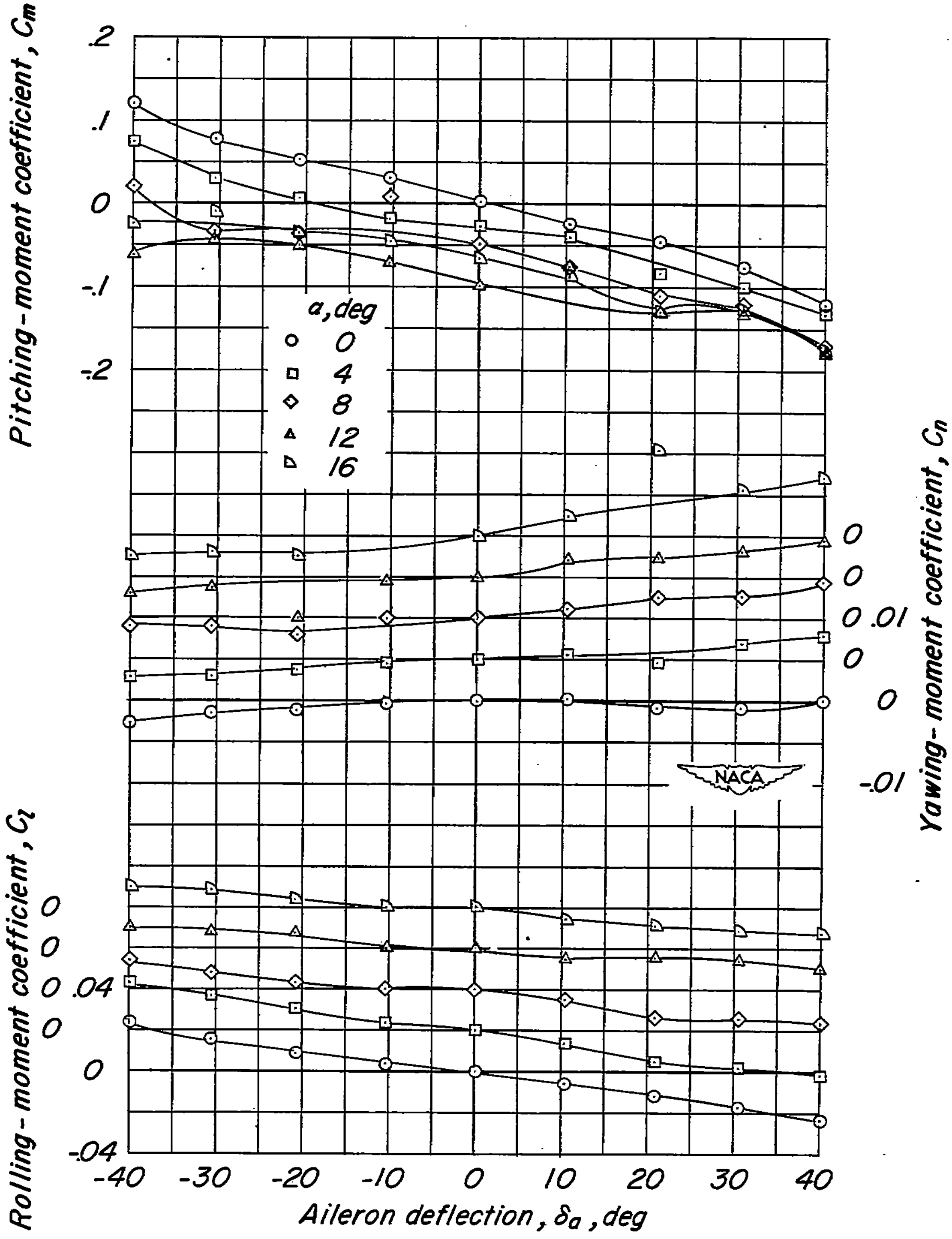

(f) Concluded.

Figure 7.- Continued.

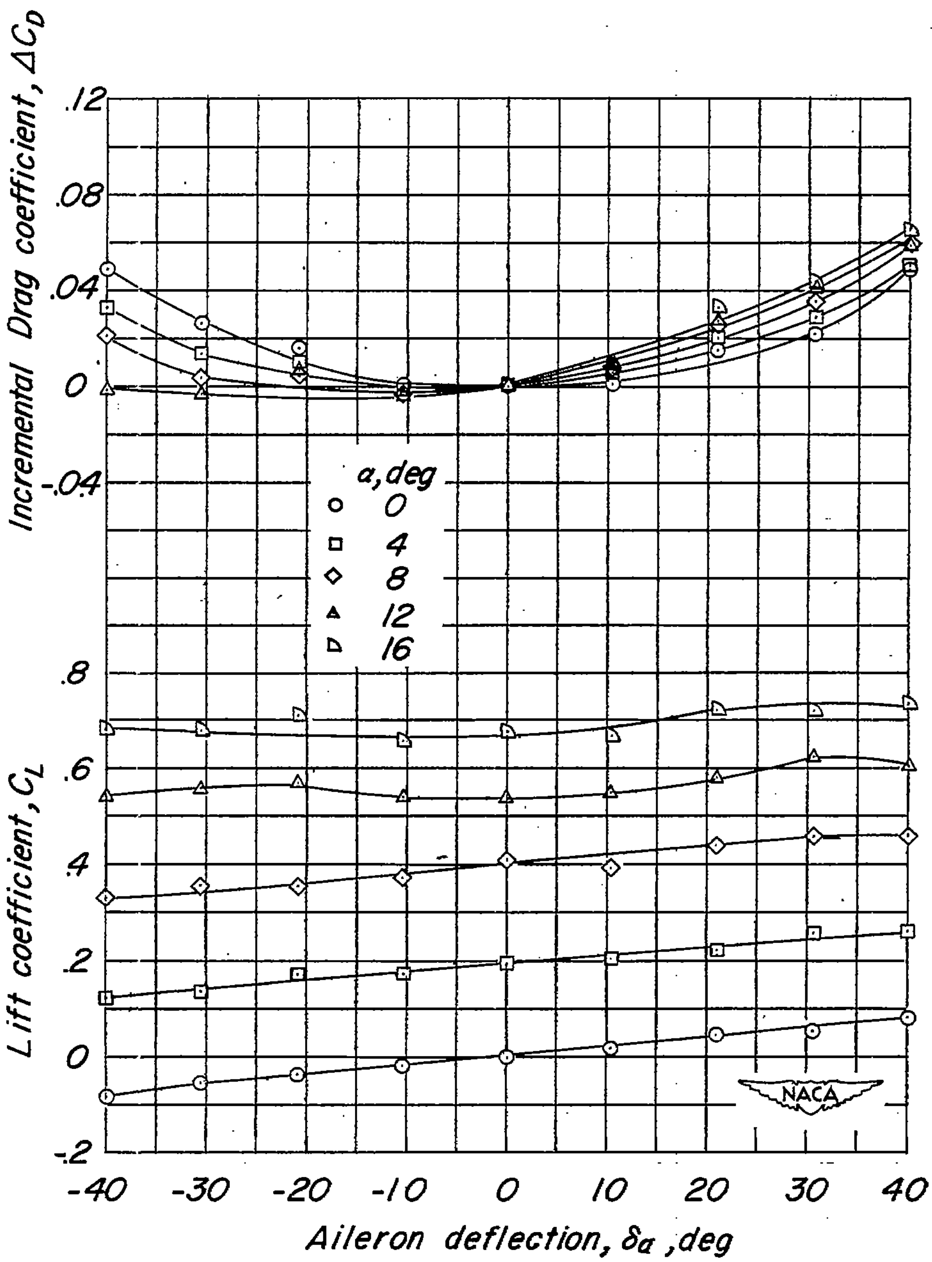

(g) M = 1.15.

Figure 7.- Continued.

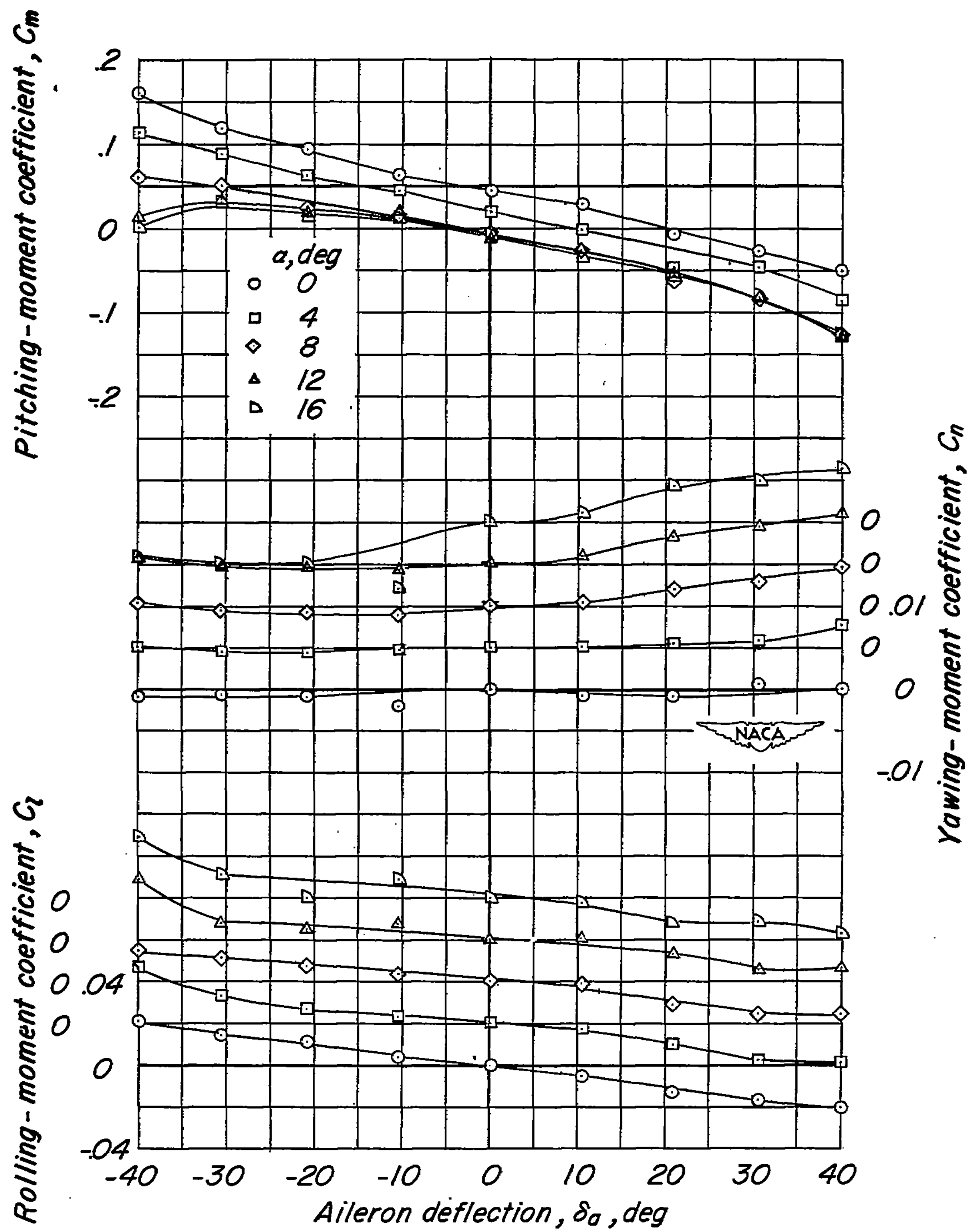

(g) Concluded.

Figure 7.- Concluded.

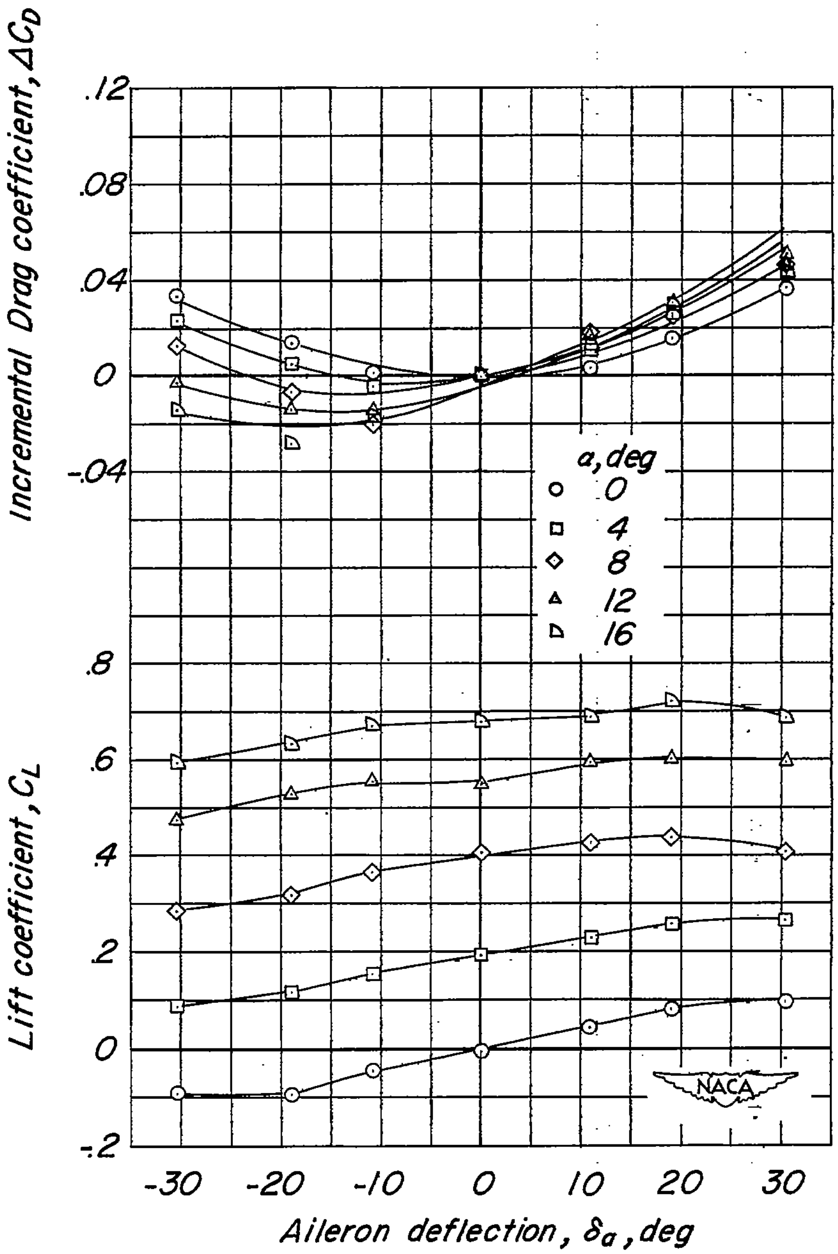

(a) M = 0.60.

Figure 8.- Aerodynamic characteristics of 51.3° sweptback wing with extended tip with triangular deflectable-tip aileron.

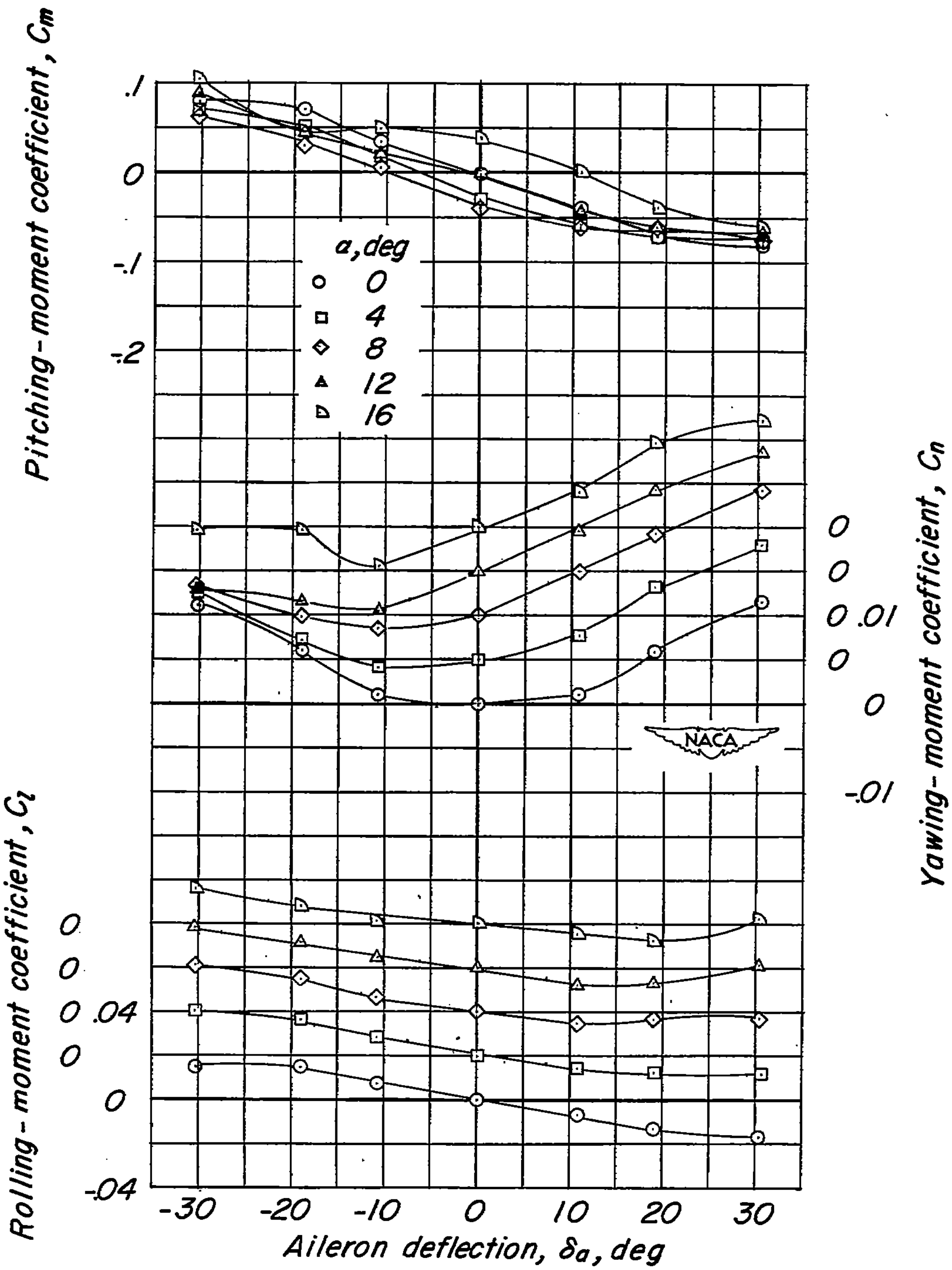

(a) Concluded.

Figure 8.- Continued.

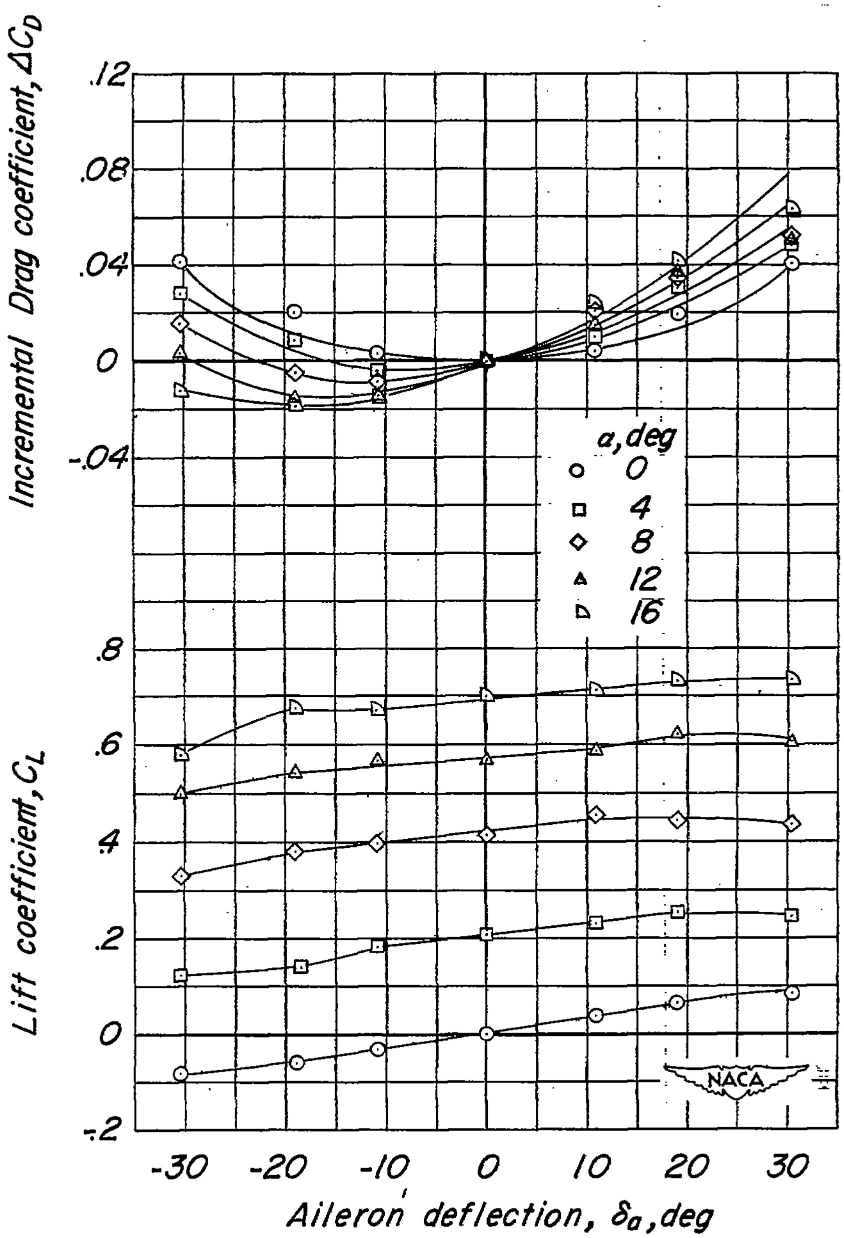

(b) M = 0.80.

Figure 8.- Continued.

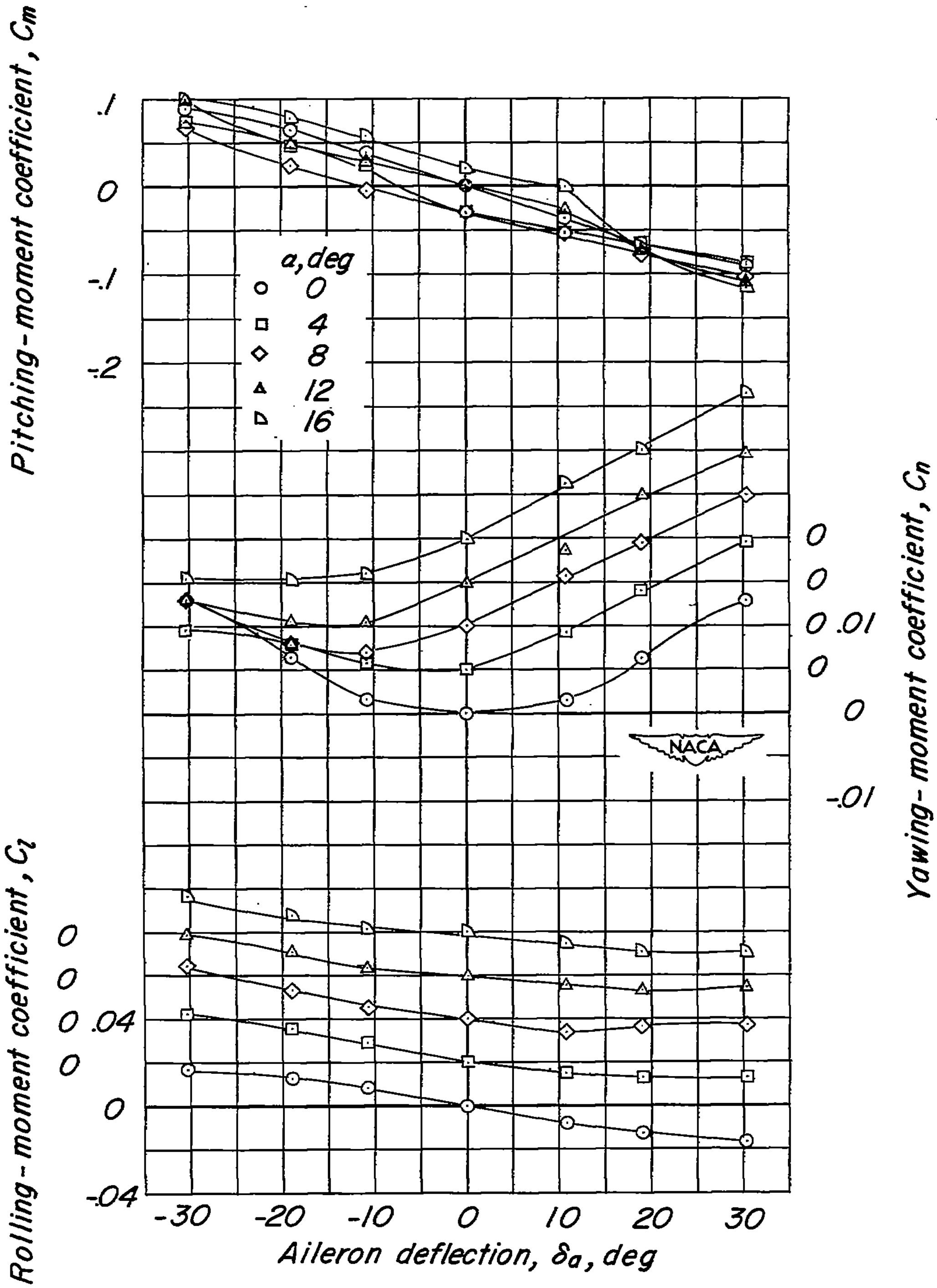

(b) Concluded.

Figure 8.- Continued.

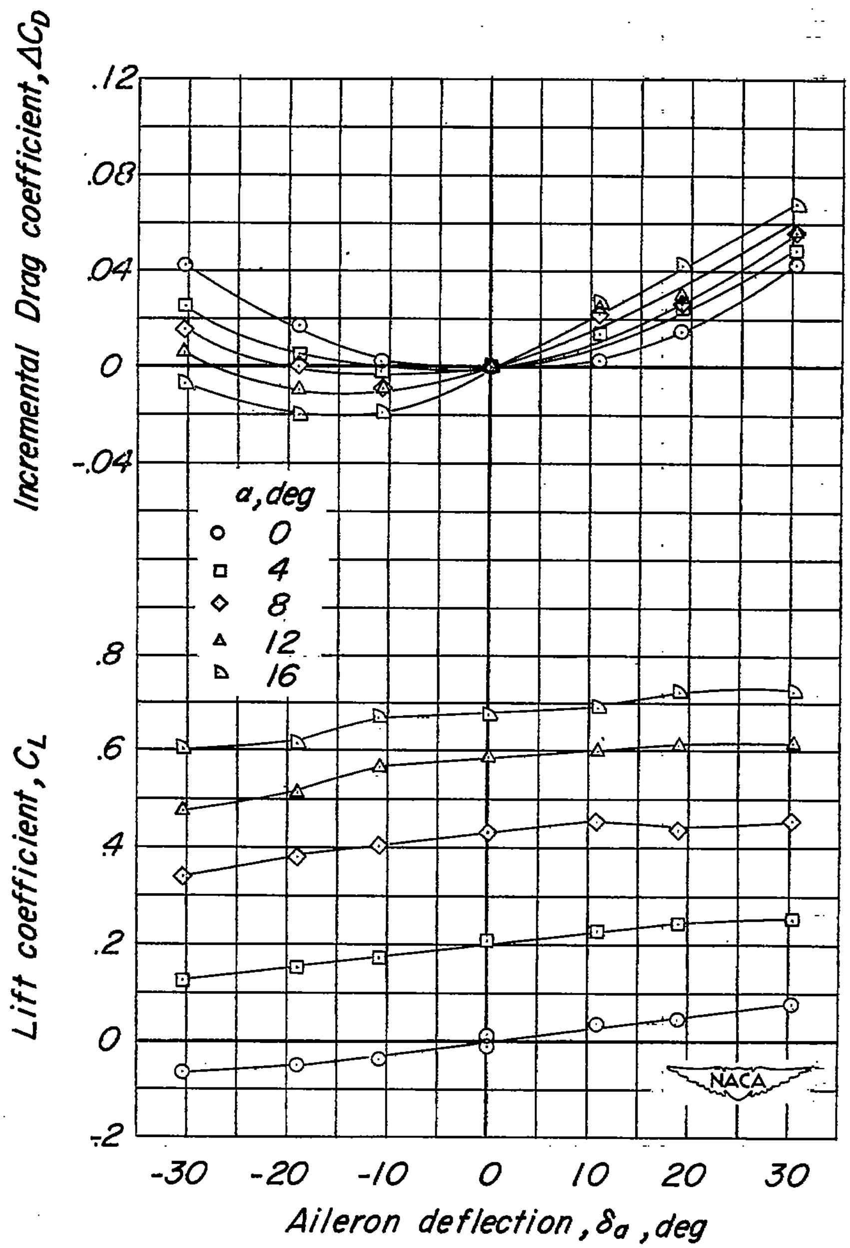

(c) M = 0.90.

Figure 8.- Continued.

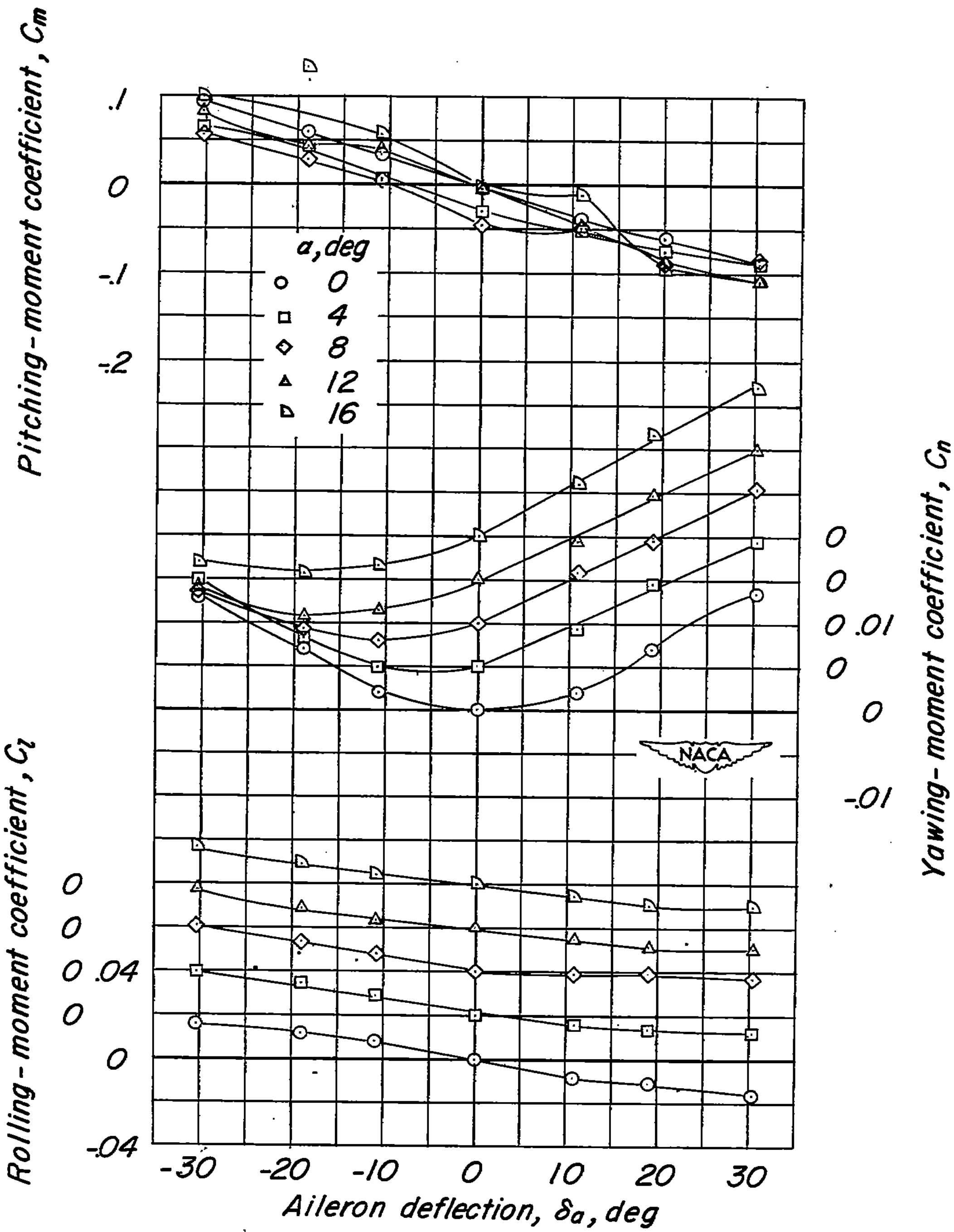

(c) Concluded.

Figure 8.- Continued.

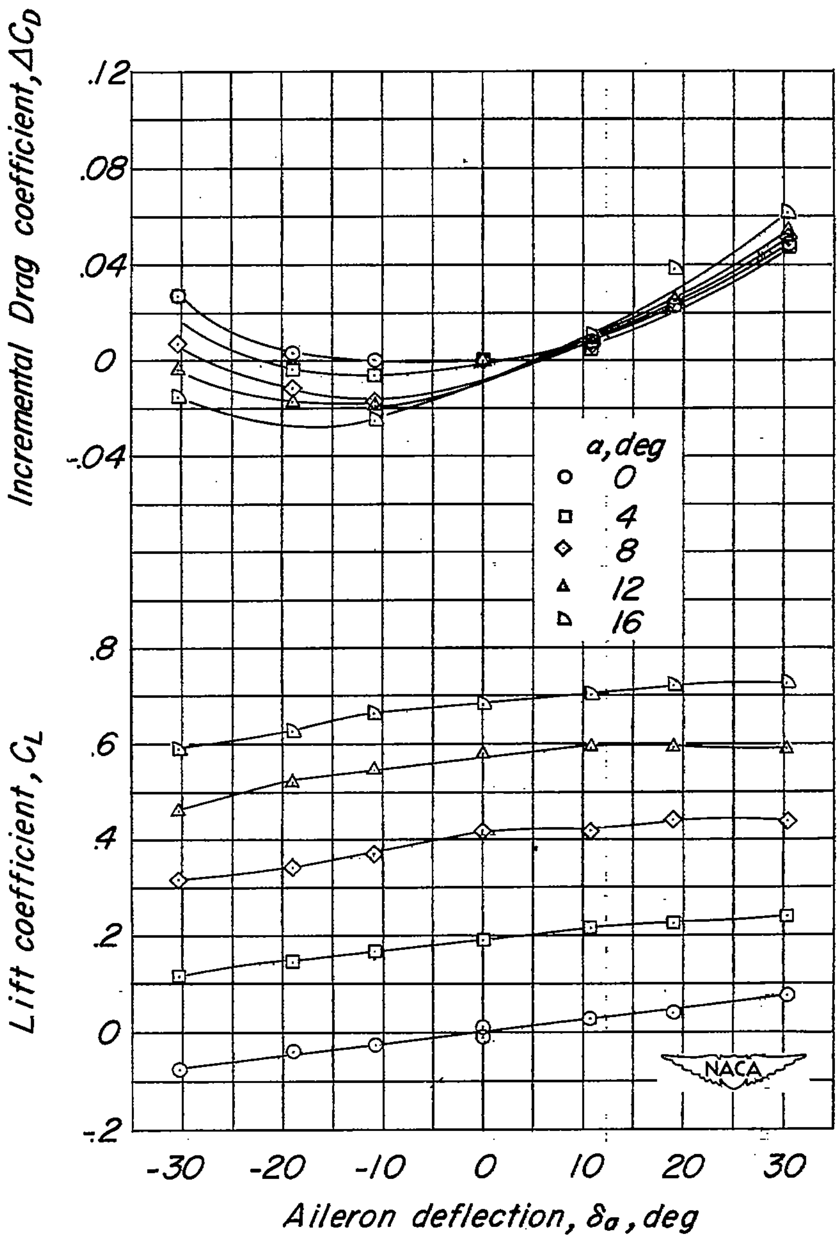

(d) M = 0.95.

Figure 8.- Continued.

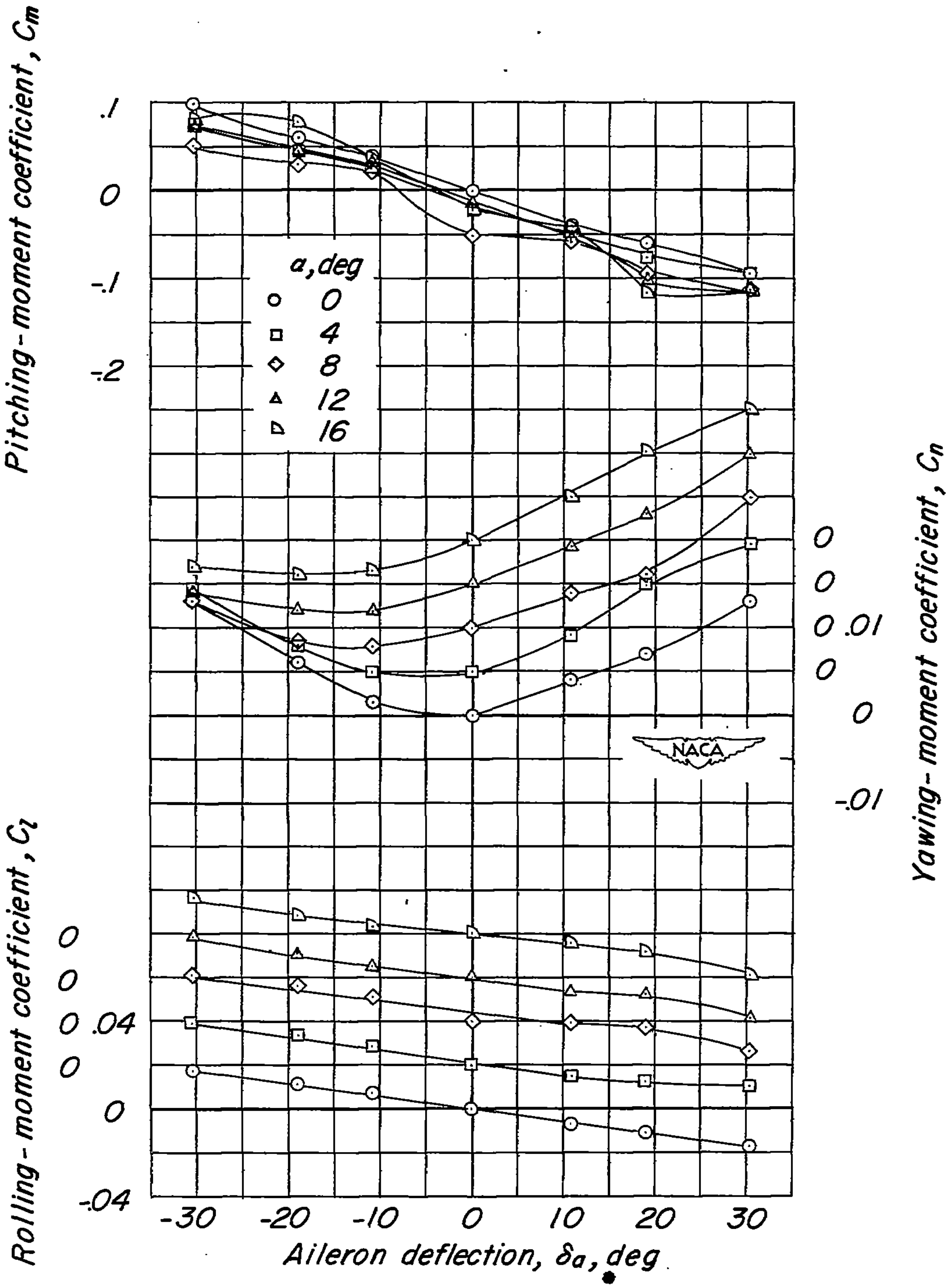

(d) Concluded.

Figure 8.- Continued.

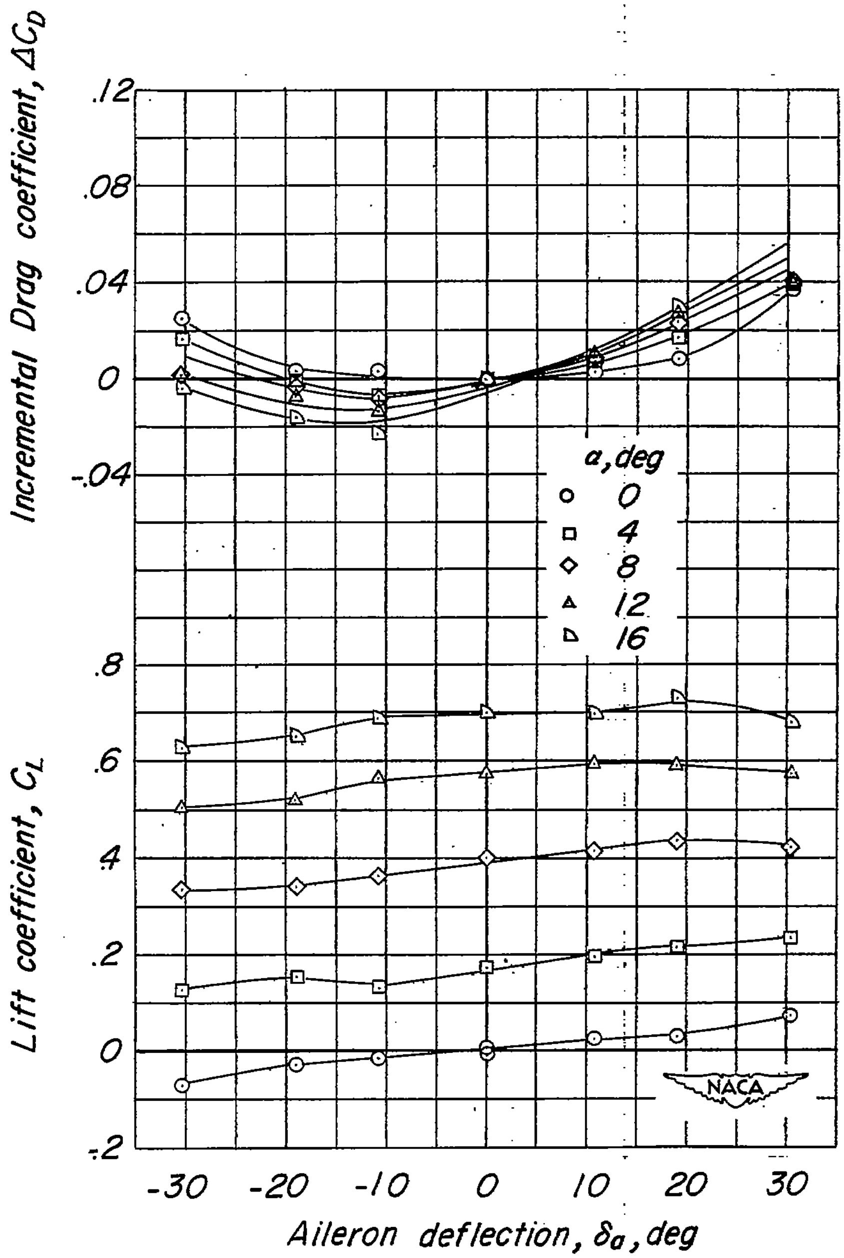

(e) M = 1.00.

Figure 8.- Continued.

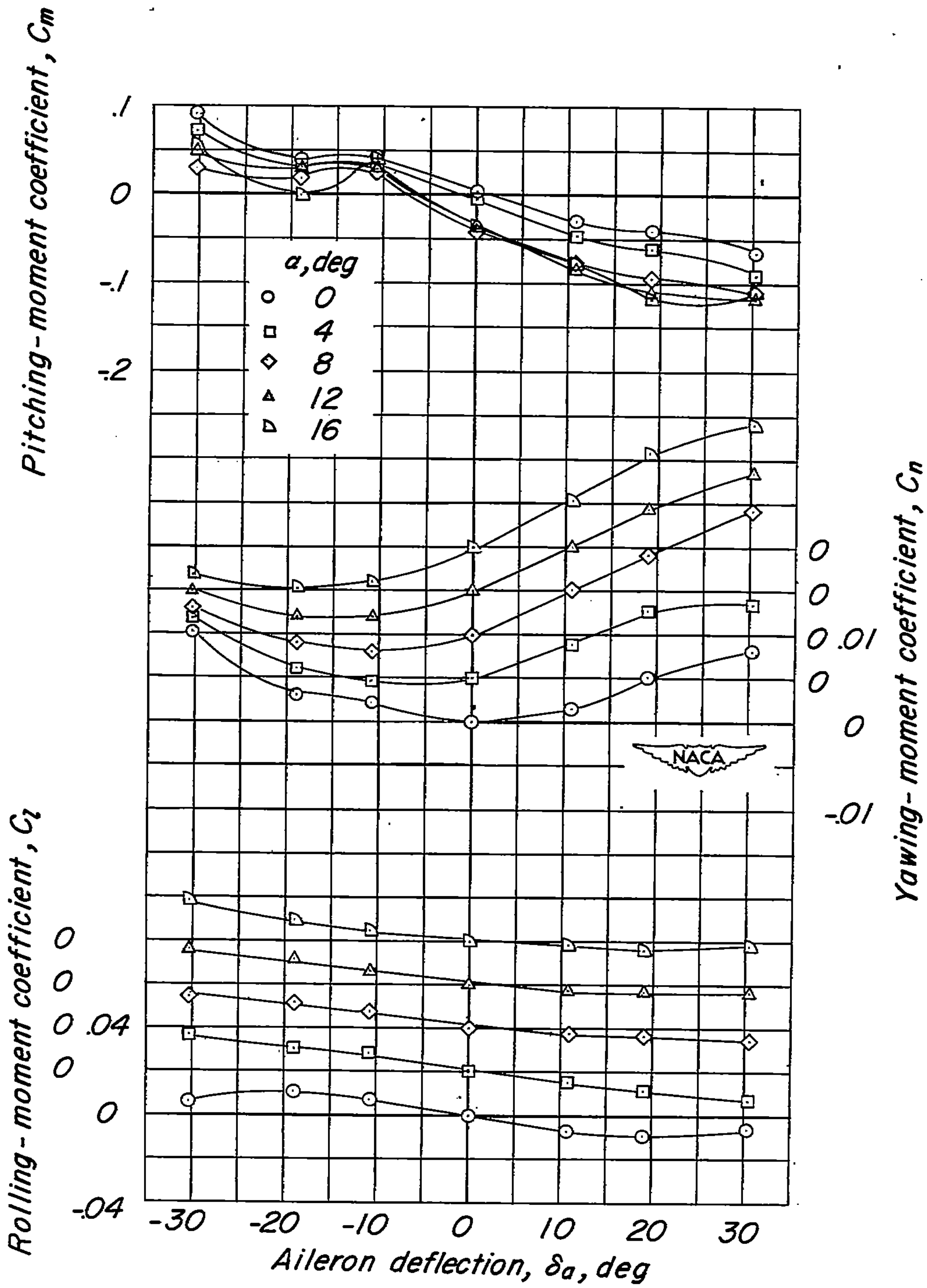

(e) Concluded.

Figure 8.- Continued.

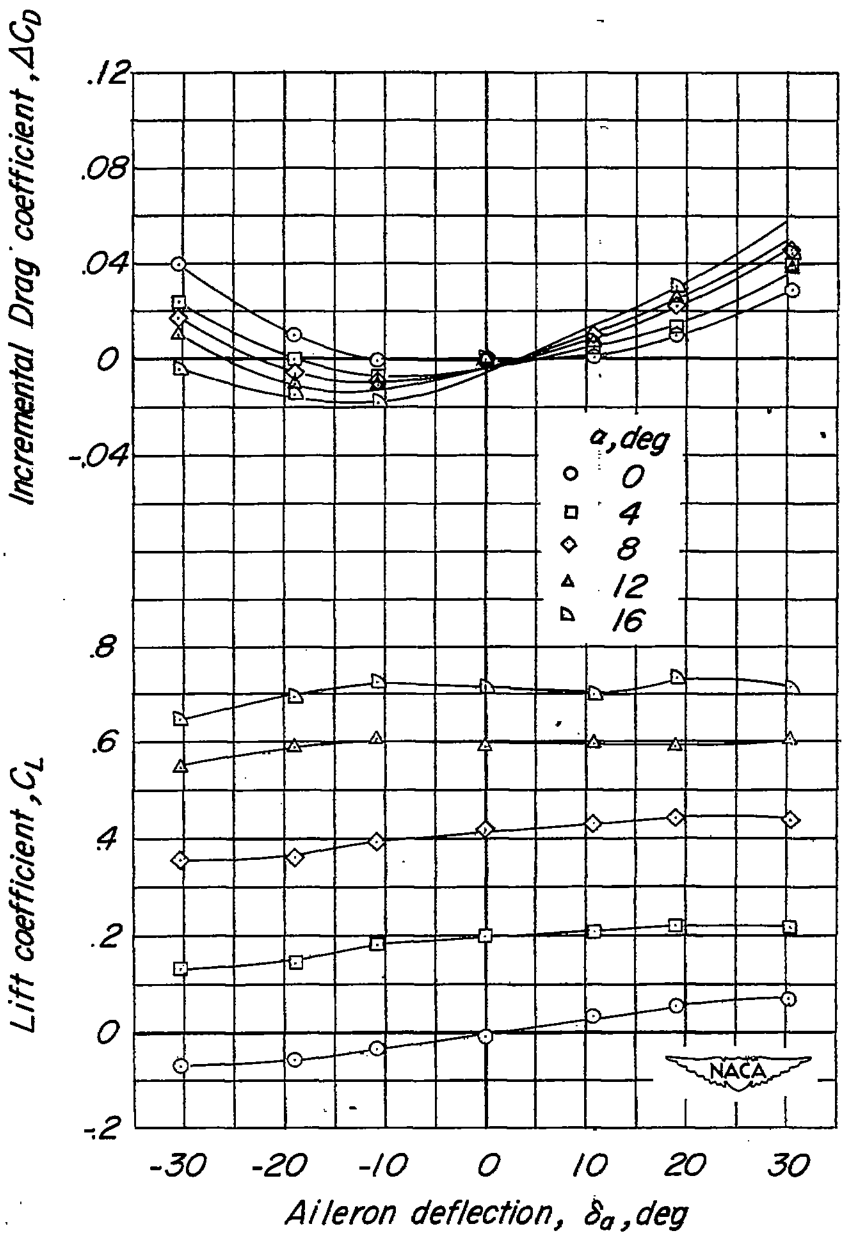

(f) M = 1.05.

Figure 8.- Continued.

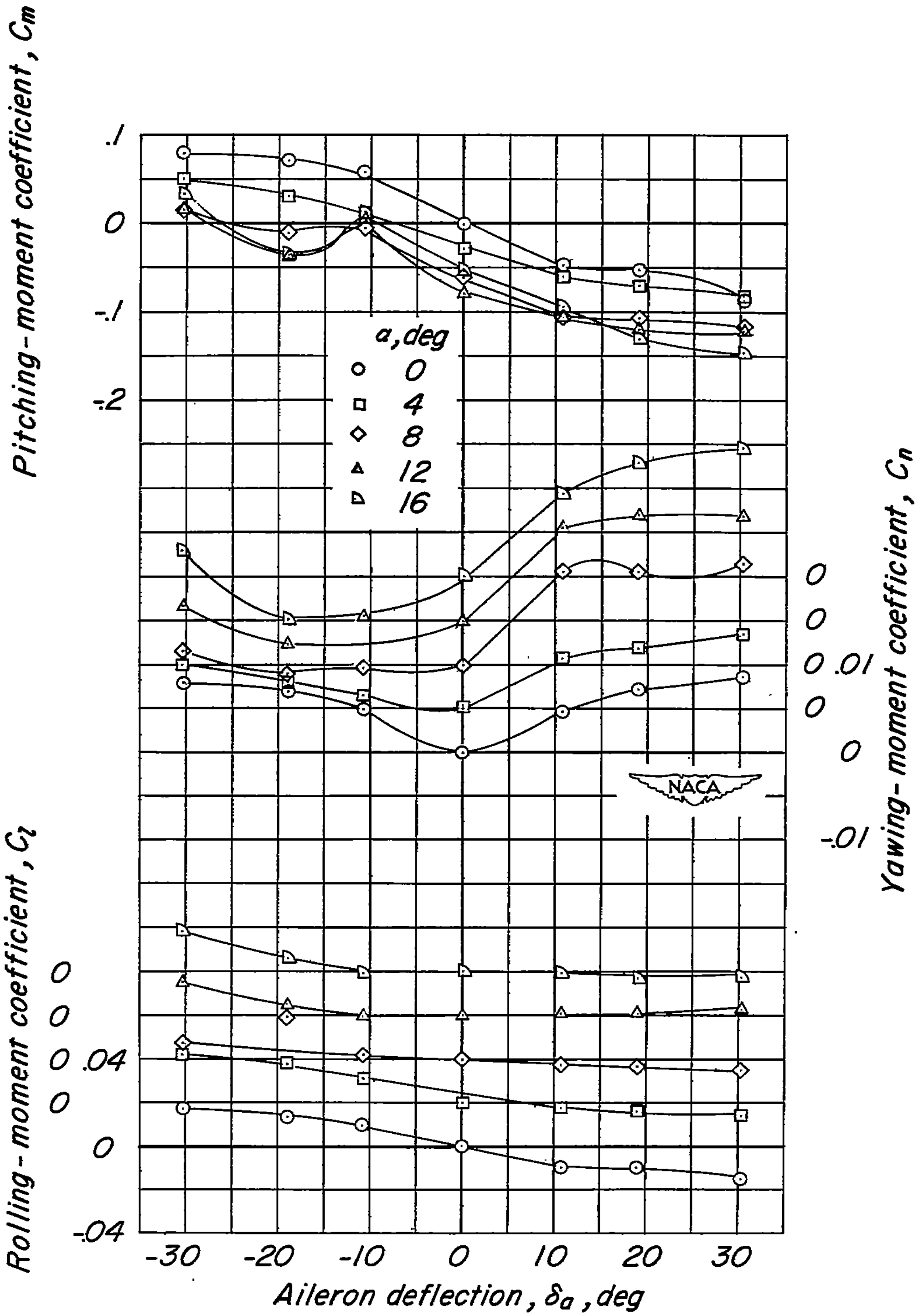

(f) Concluded.

Figure 8.- Continued.

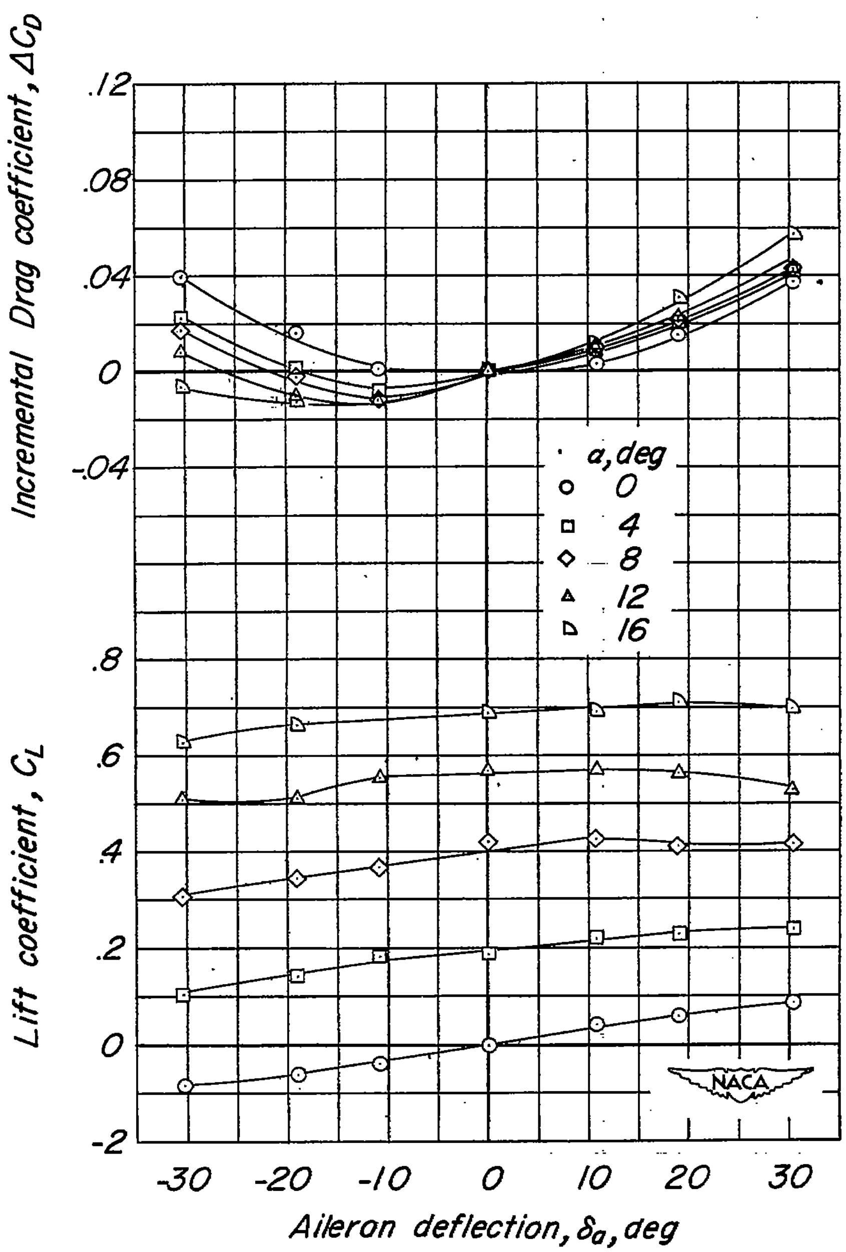

(g) M = 1.15.

Figure 8.- Continued.

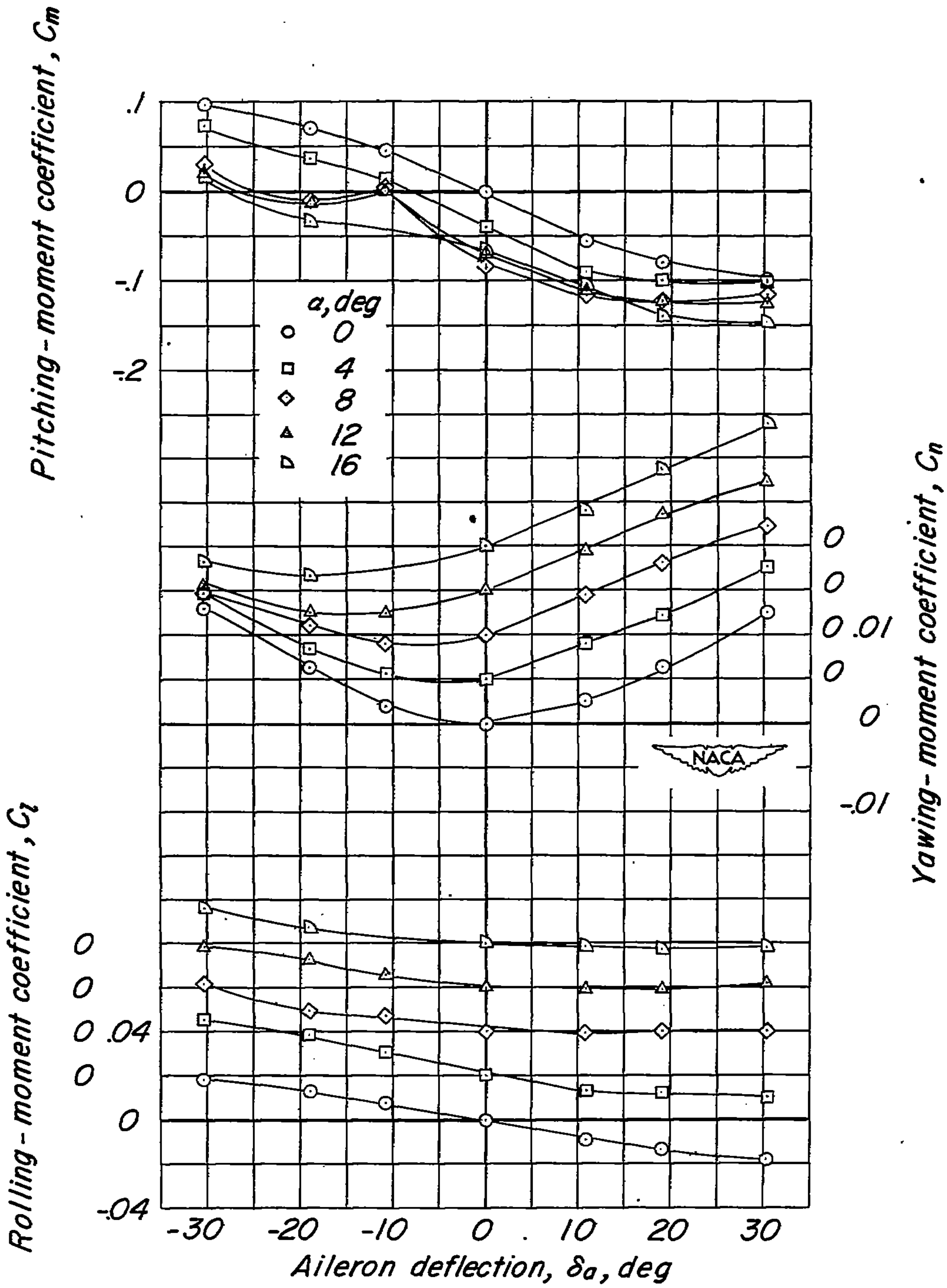

(g) Concluded.

Figure 8.- Concluded.

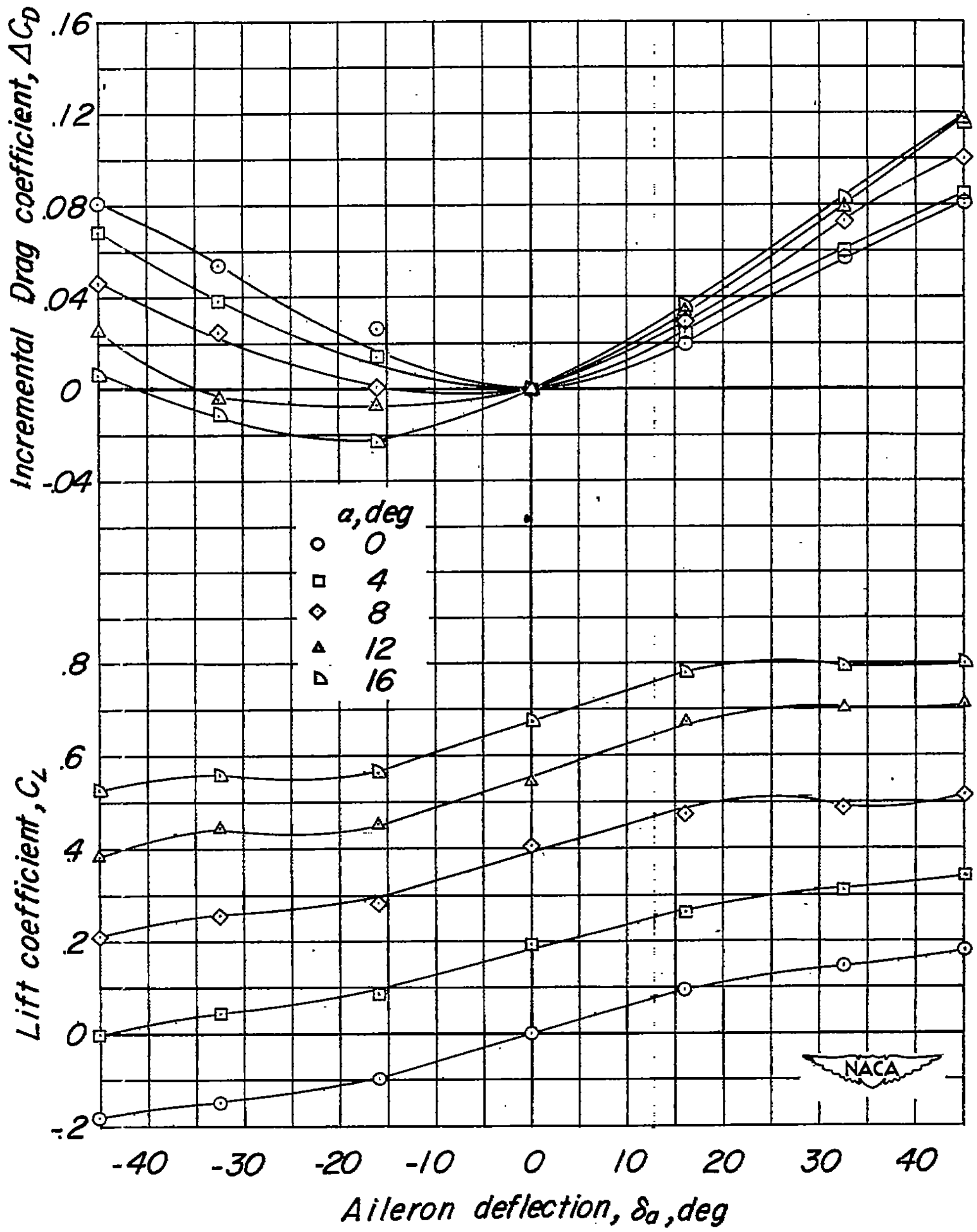

(a) M = 0.60.

Figure 9.- Aerodynamic characteristics of 51.3° sweptback wing with extended tip with trapezoidal trailing-edge aileron.

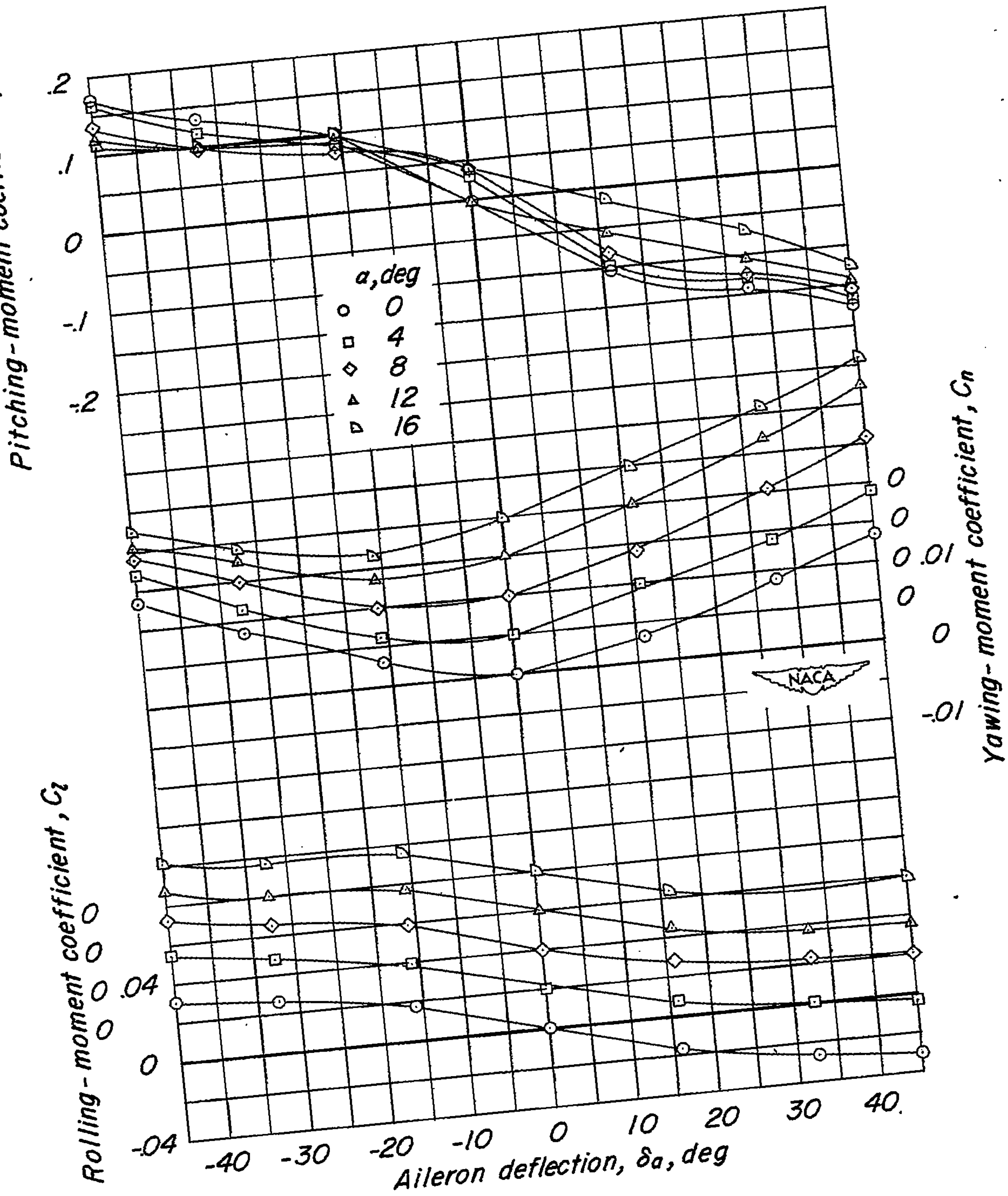

(a) Concluded.

Figure 9.- Continued.

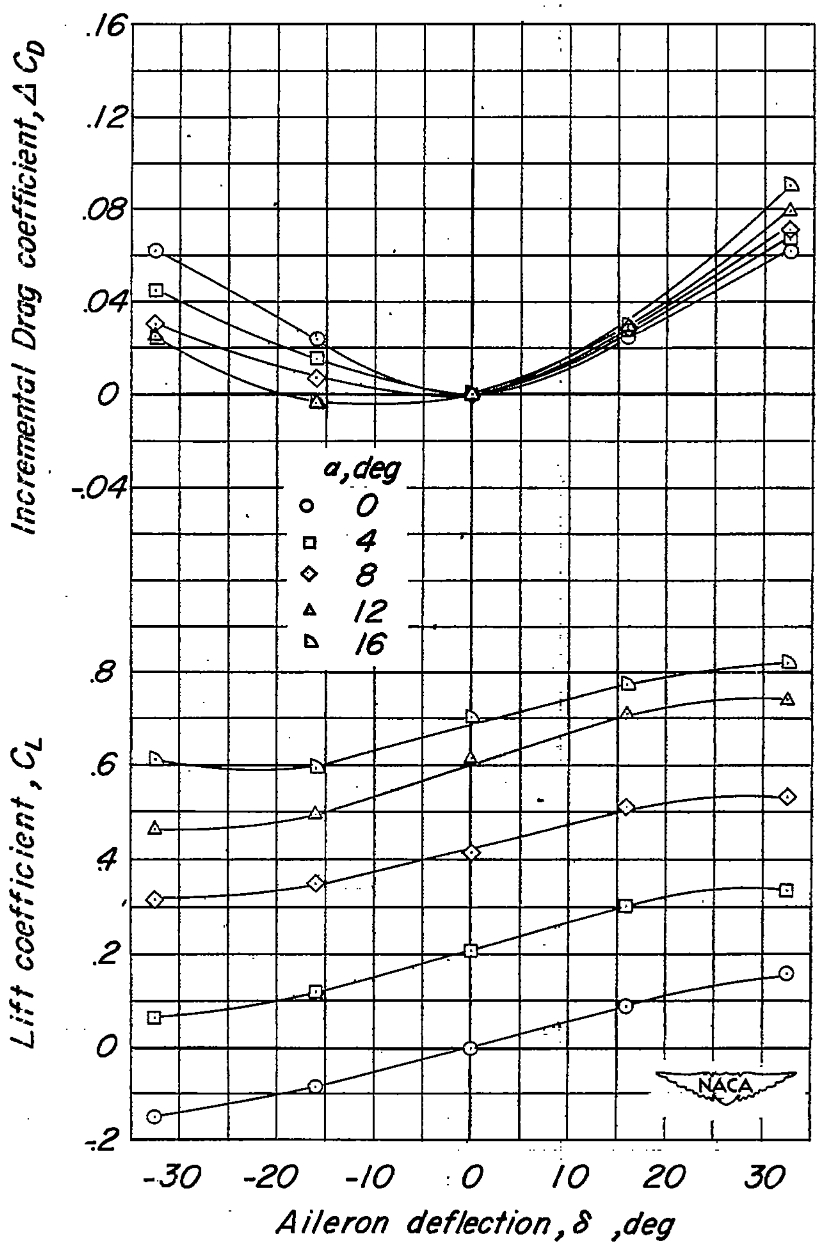

(b) M = 0.80.

Figure 9.- Continued.

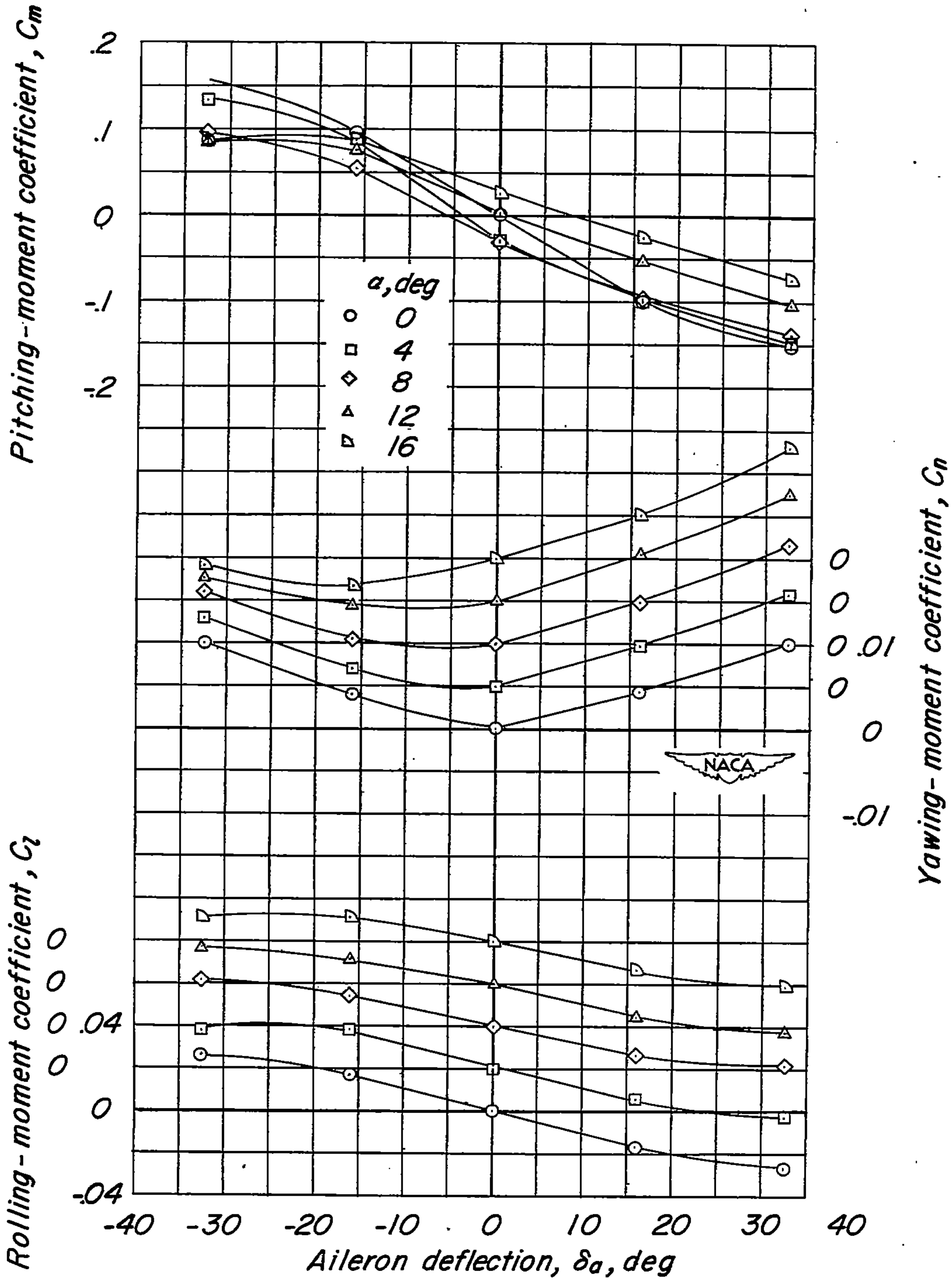

(b) Concluded.

Figure 9.- Continued.

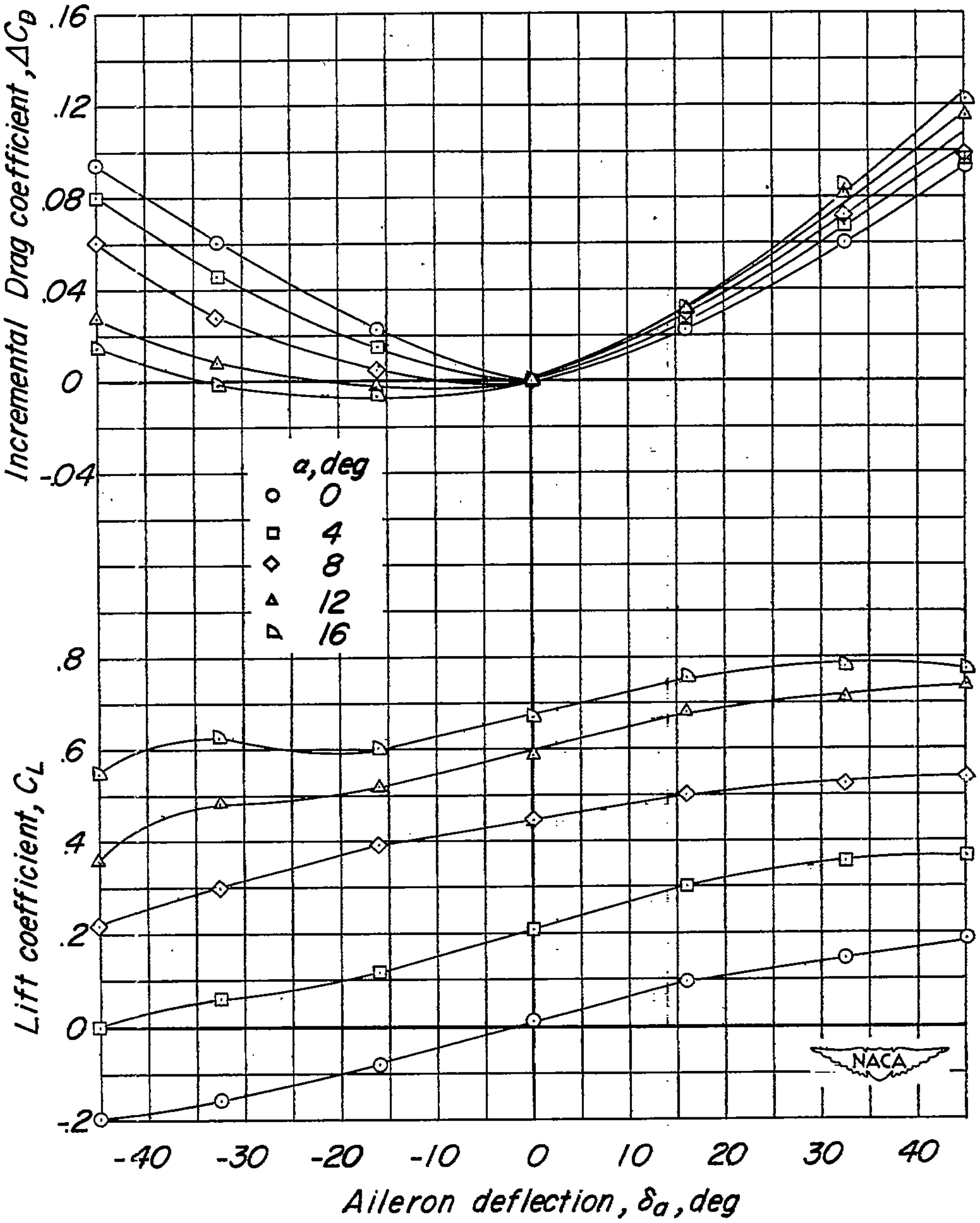

(c) M = 0.90.

Figure 9.- Continued.

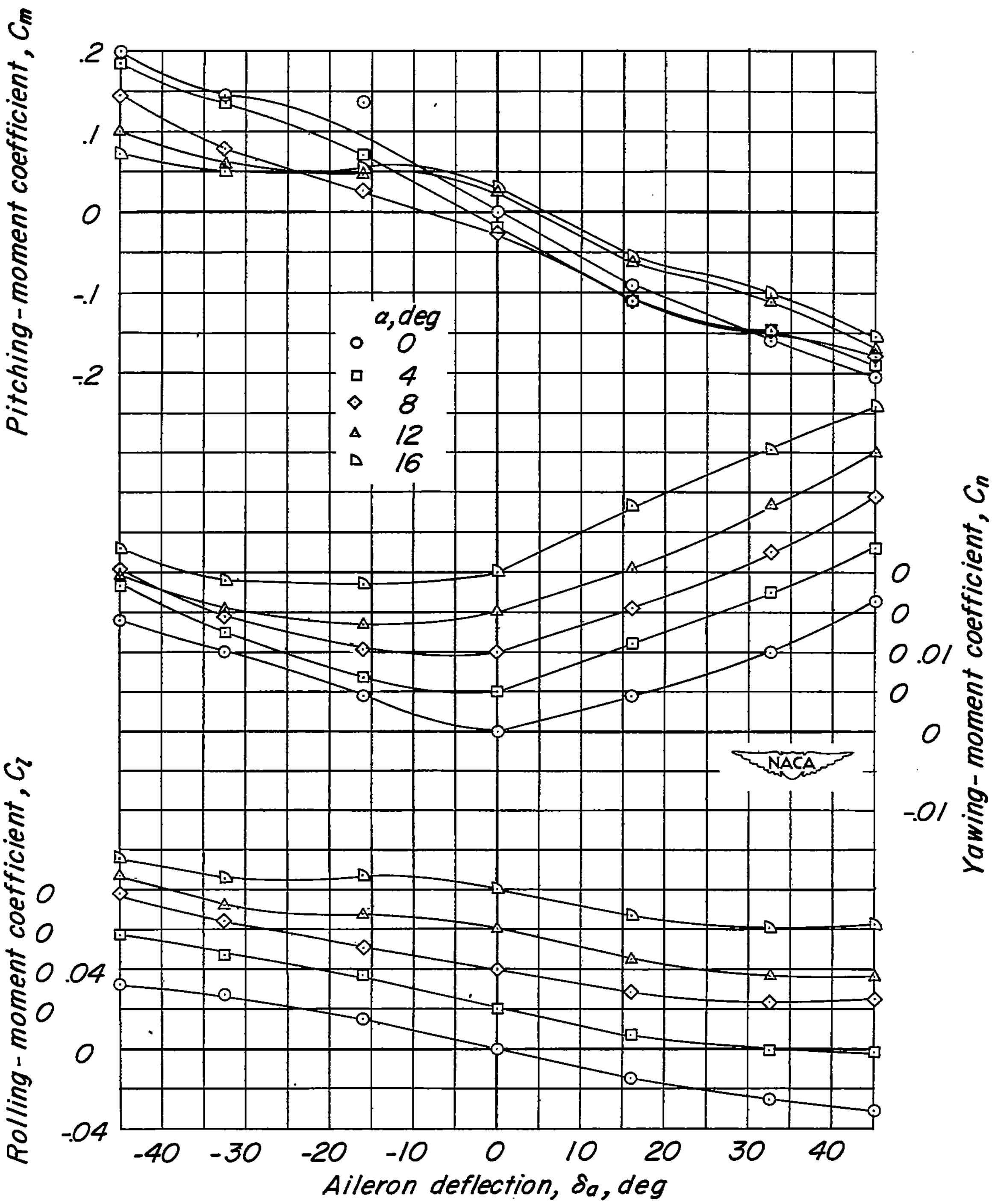

(c) Concluded.

Figure 9.- Continued.

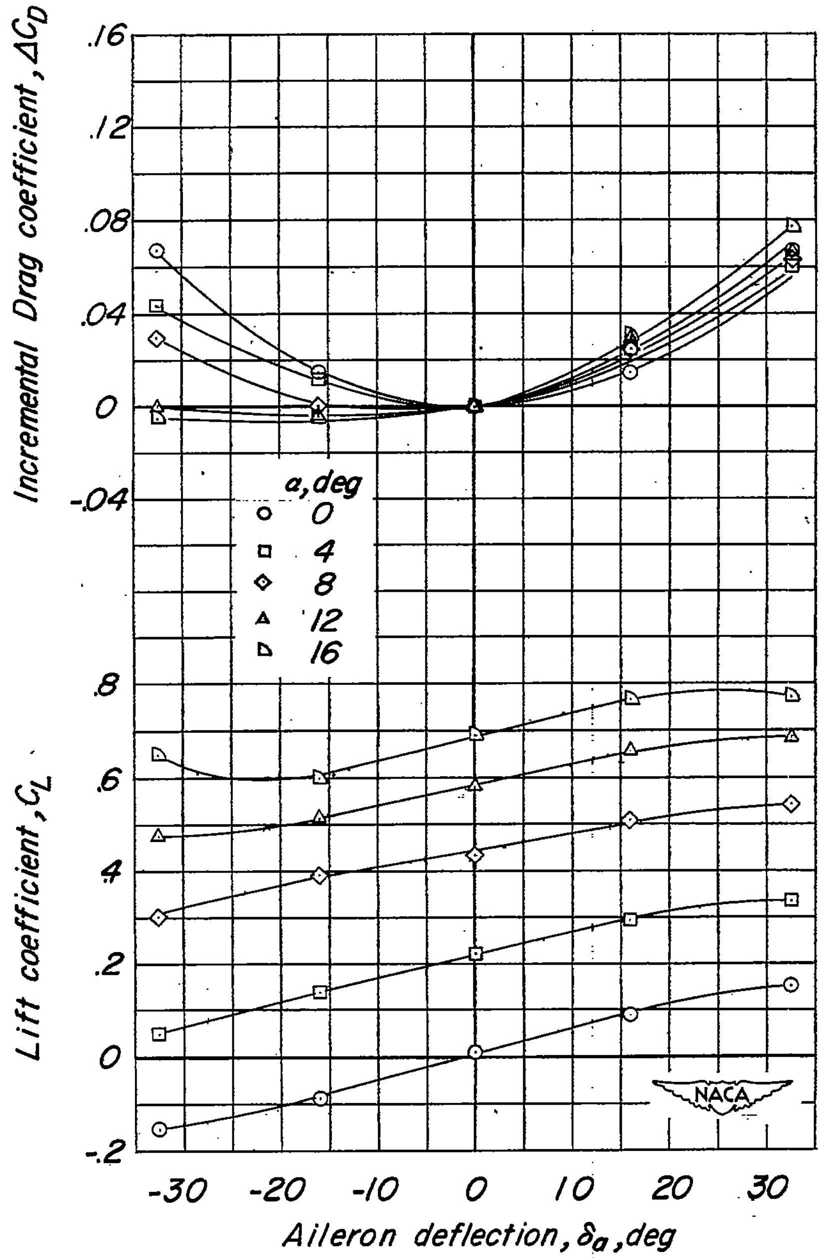

(d) M = 0.95.

Figure 9.- Continued.

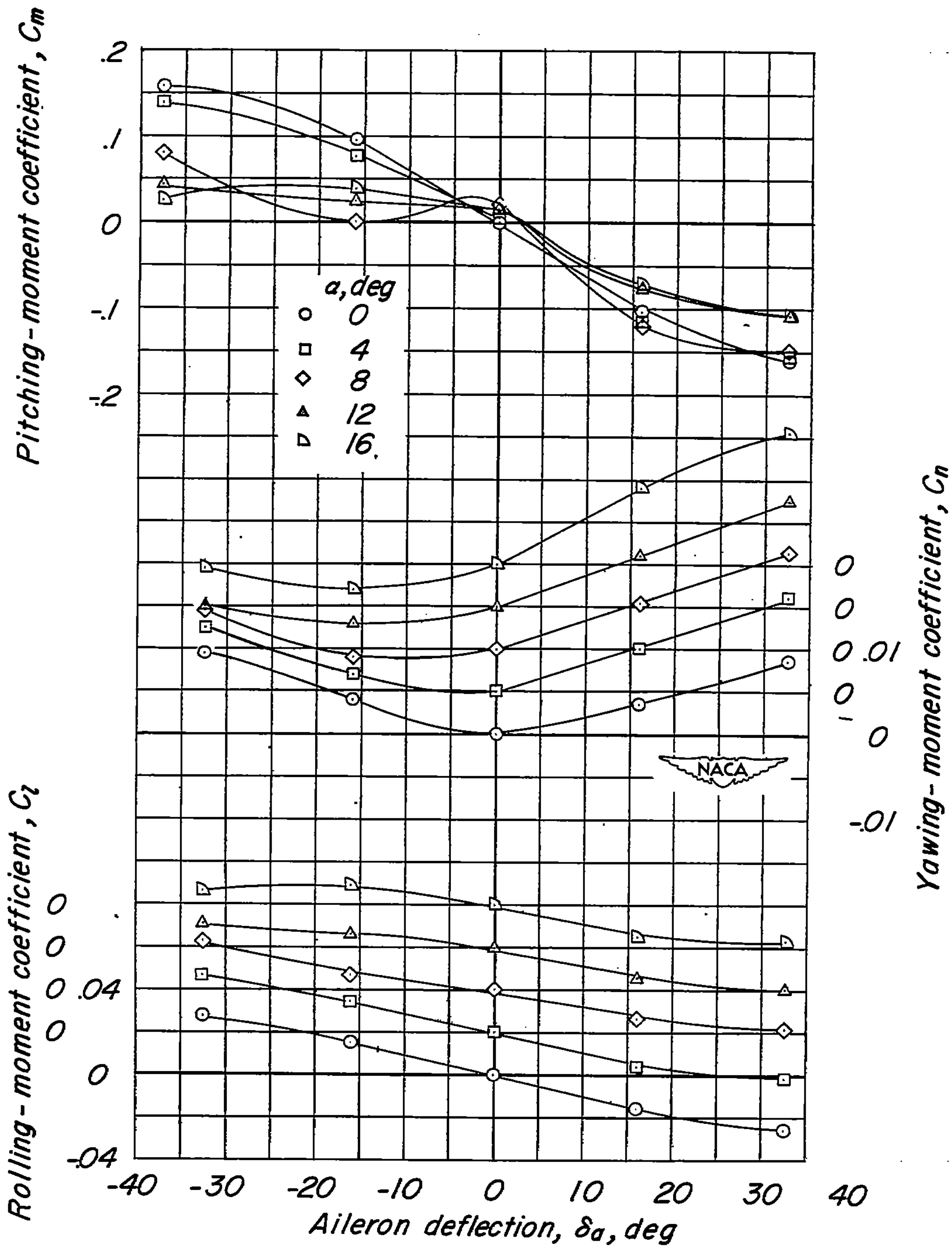

(d) Concluded.

Figure 9.- Continued.

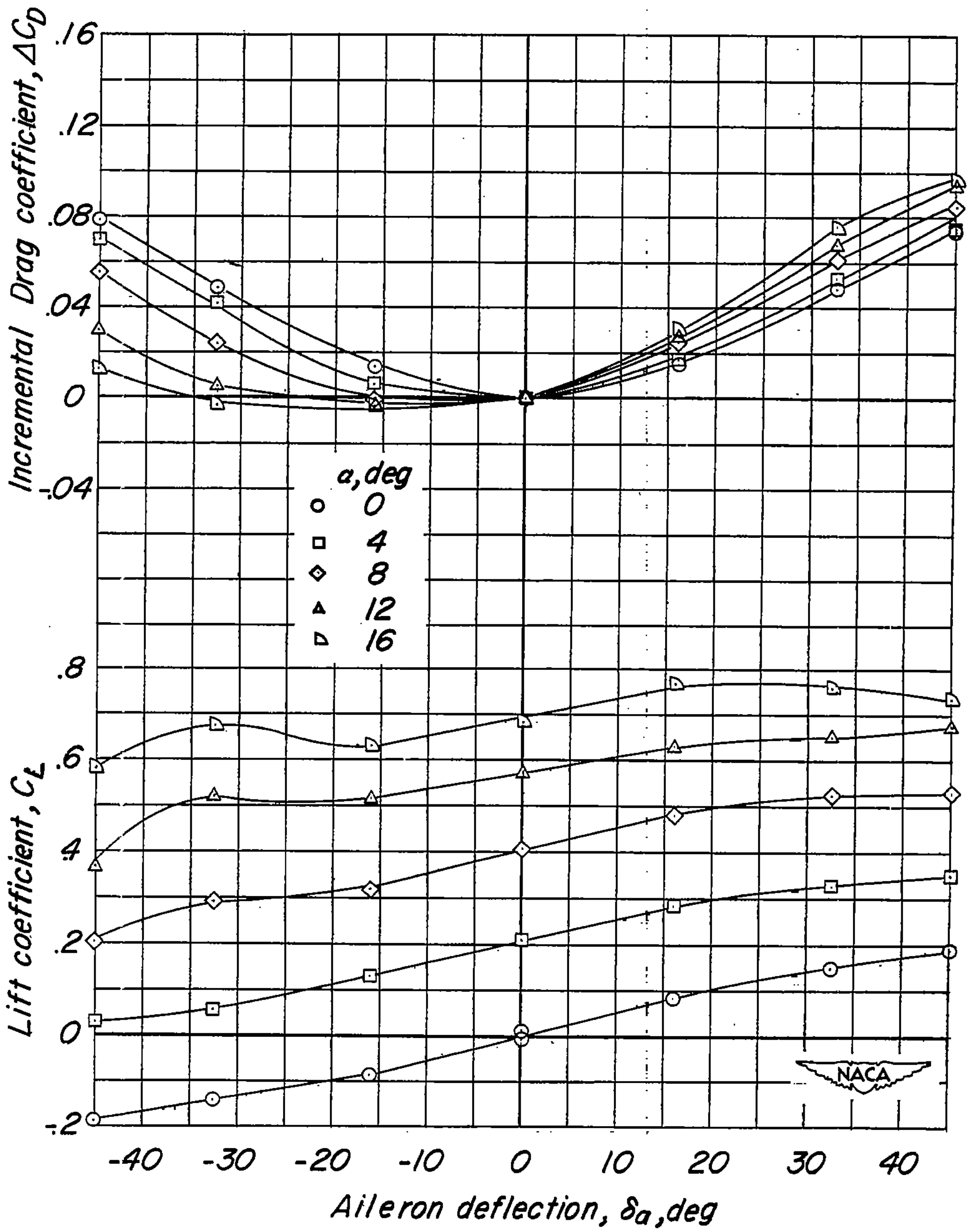

(e) M = 1.00.

Figure 9.- Continued.

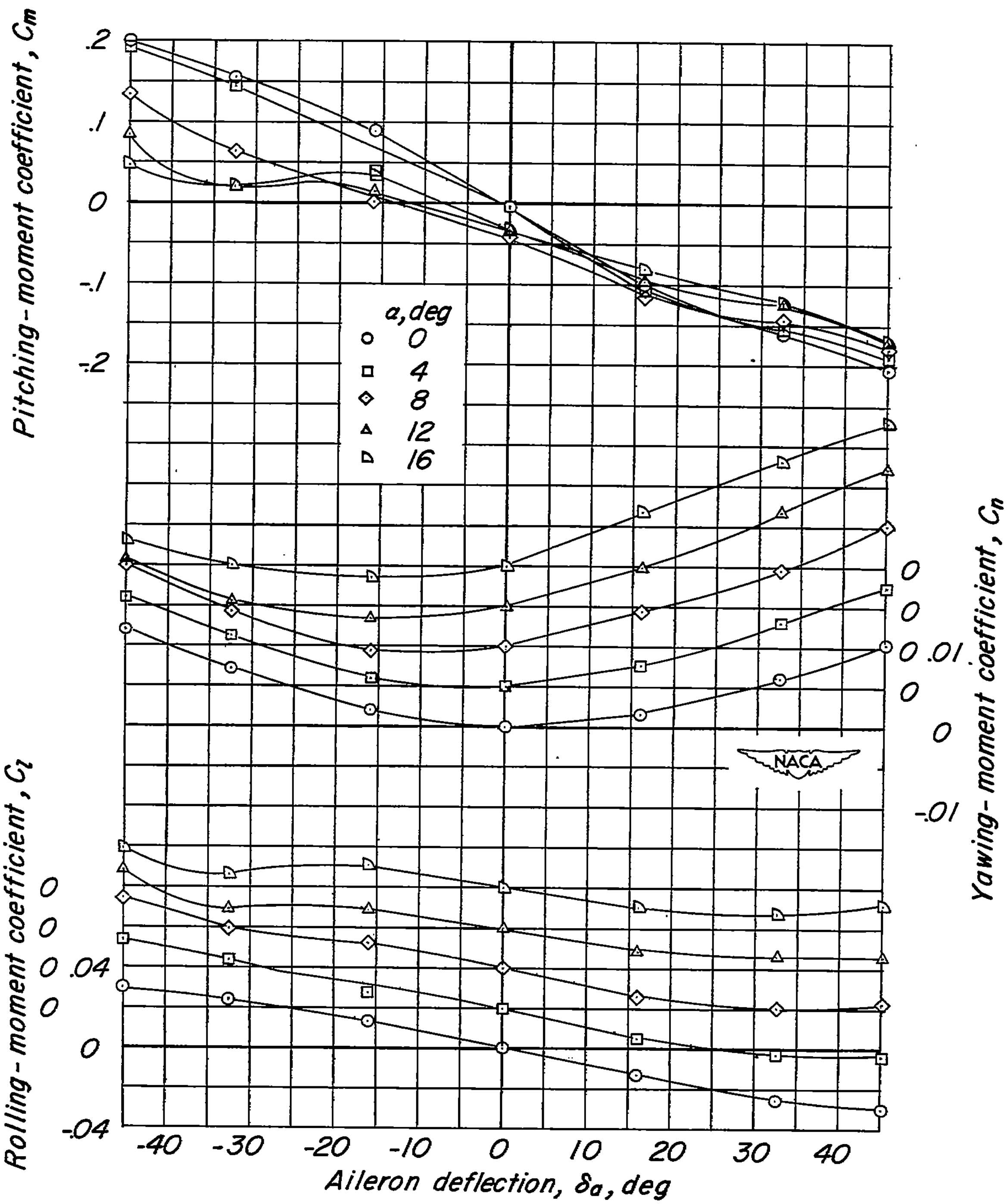

(e) Concluded.

Figure 9.- Continued.

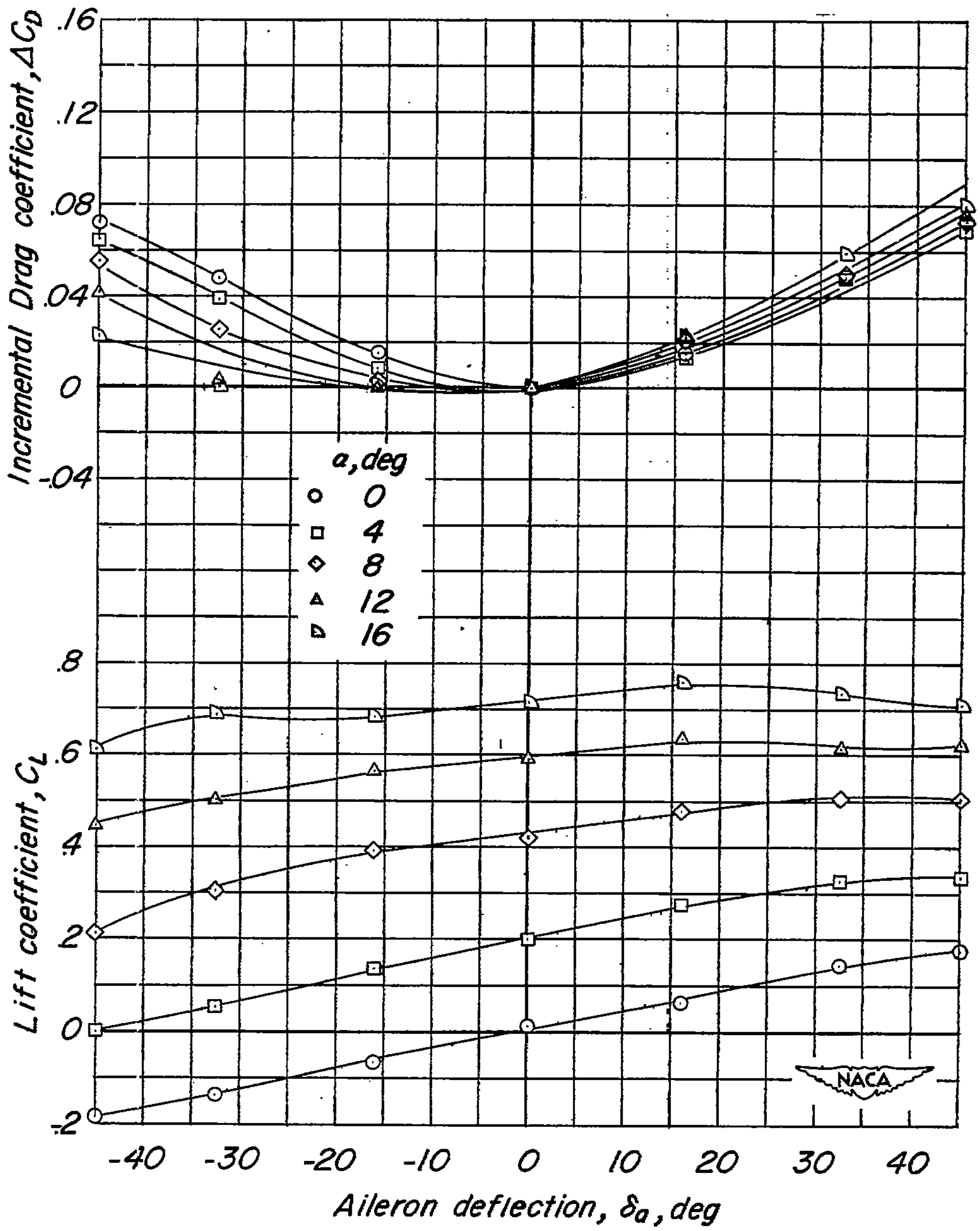

(f) M = 1.05.

Figure 9.- Continued.

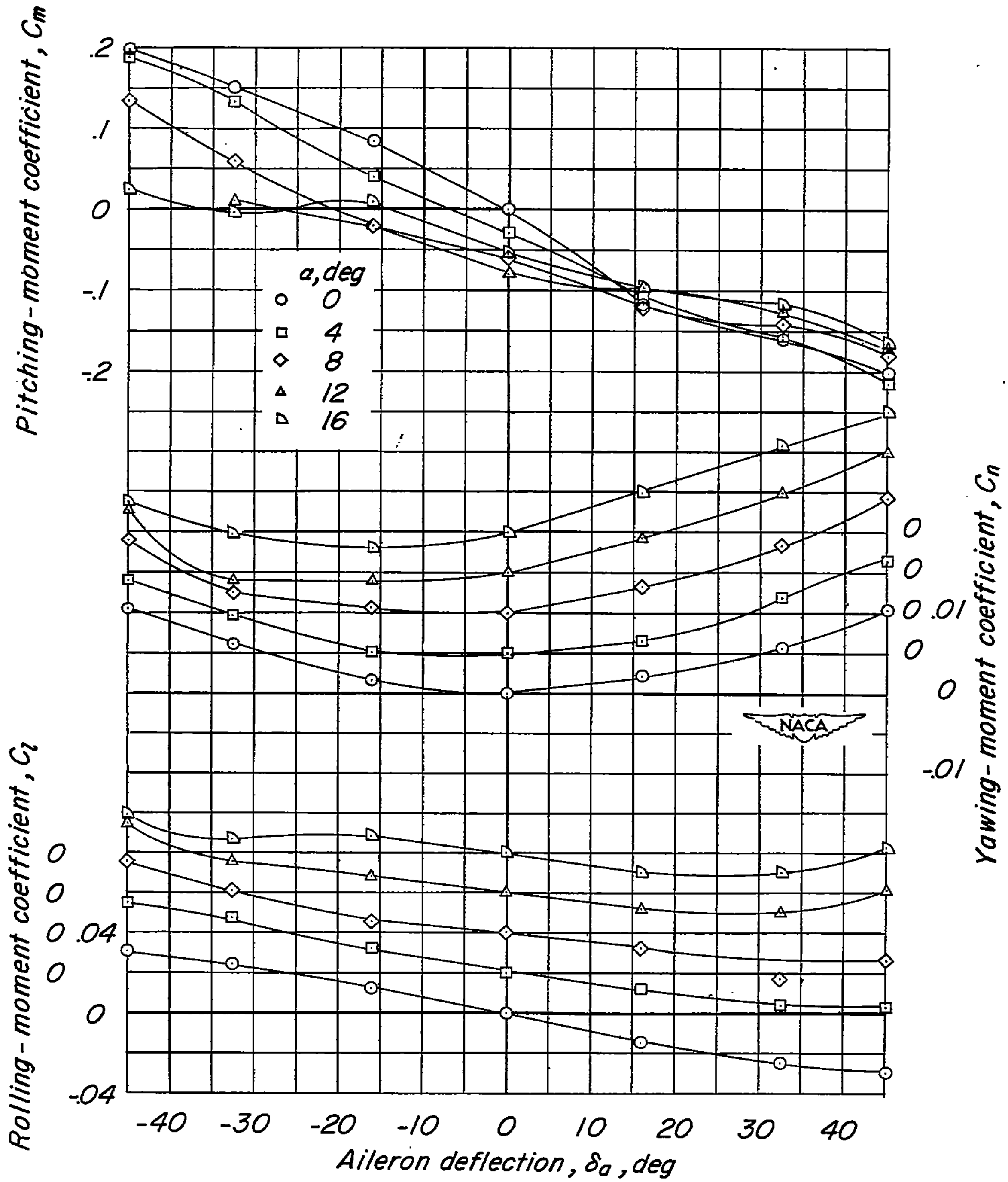

(f) Concluded.

Figure 9.- Continued.

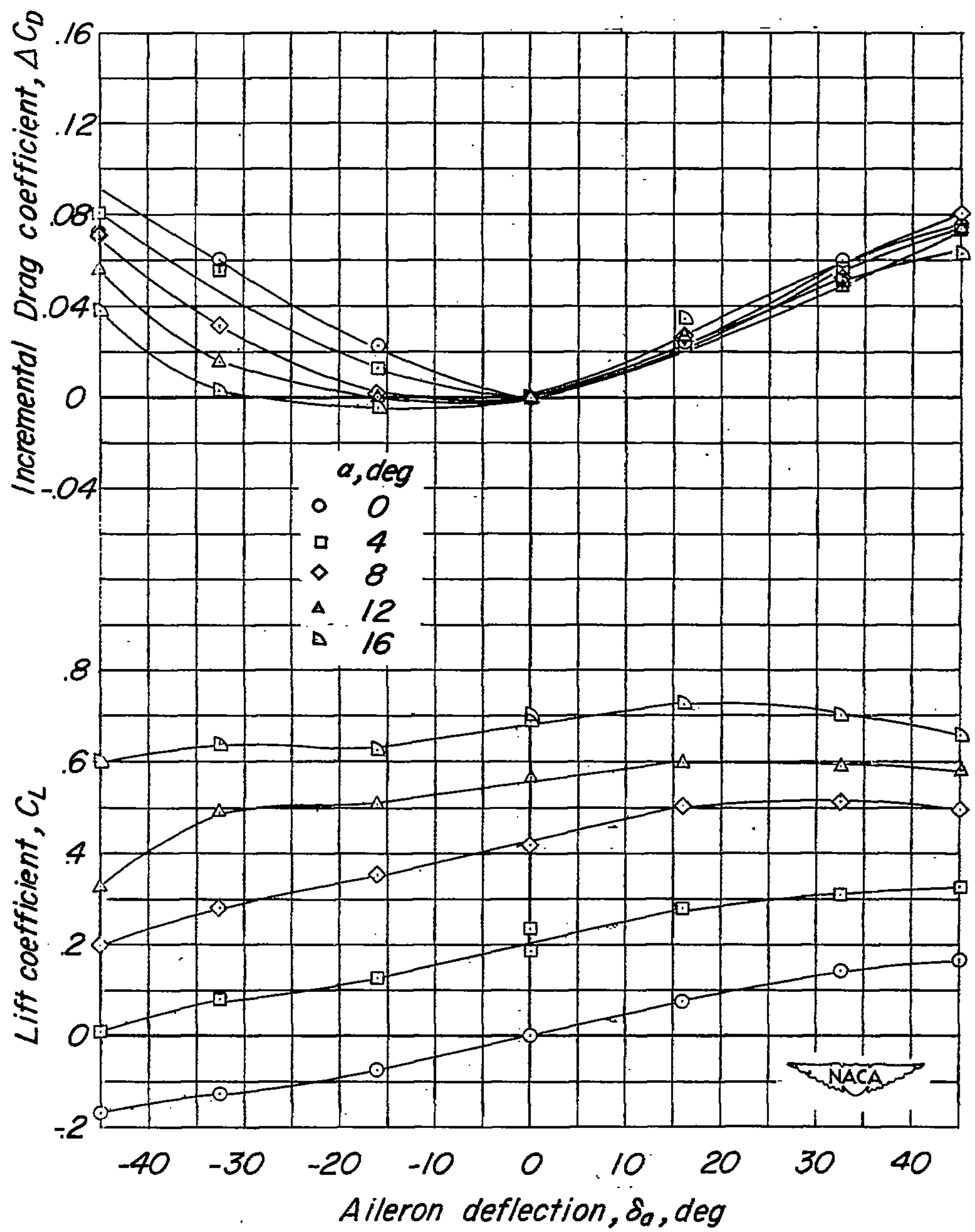

(g) M = 1.15.

Figure 9.- Continued.

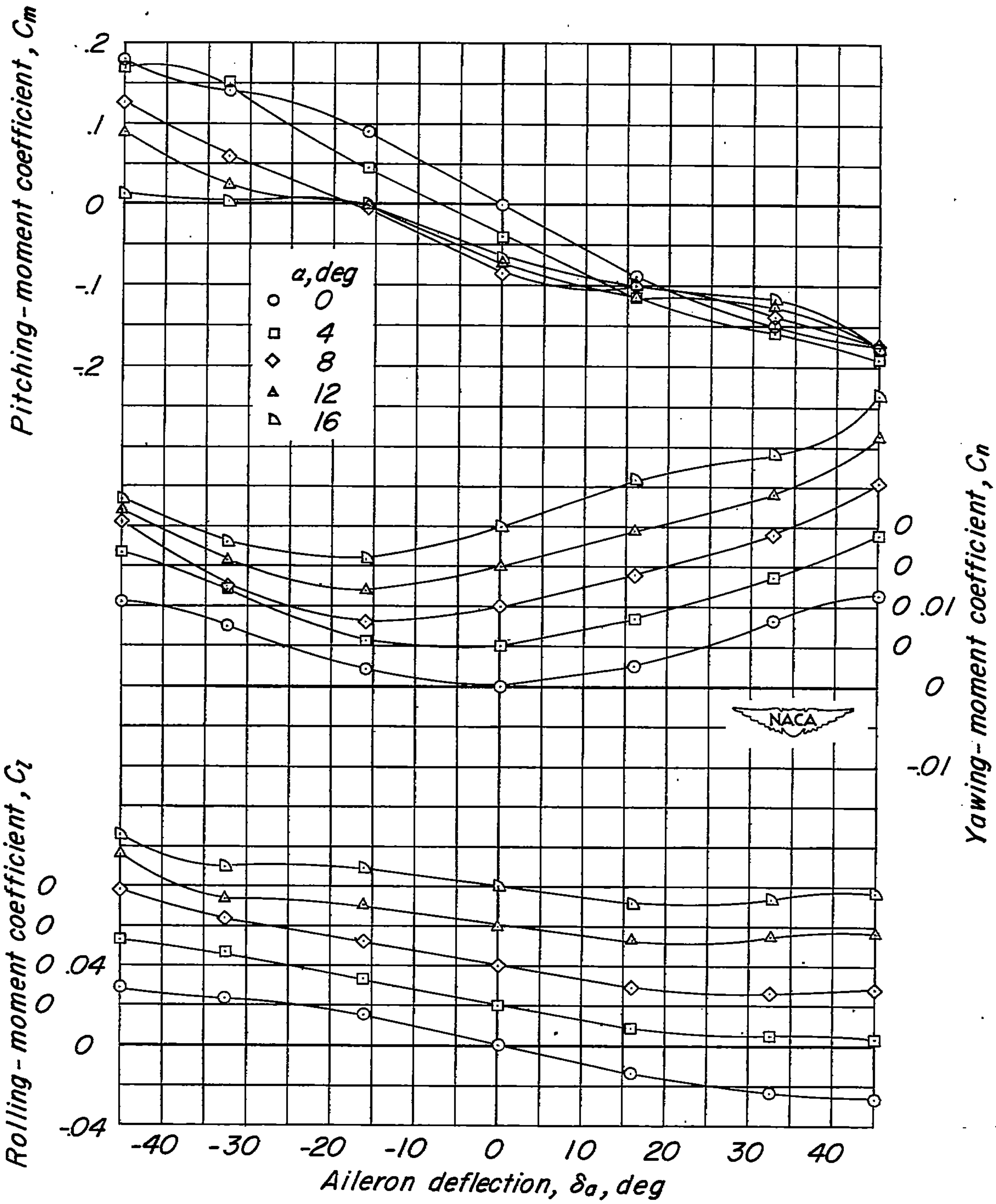

(g) Concluded.

Figure 9.- Concluded.

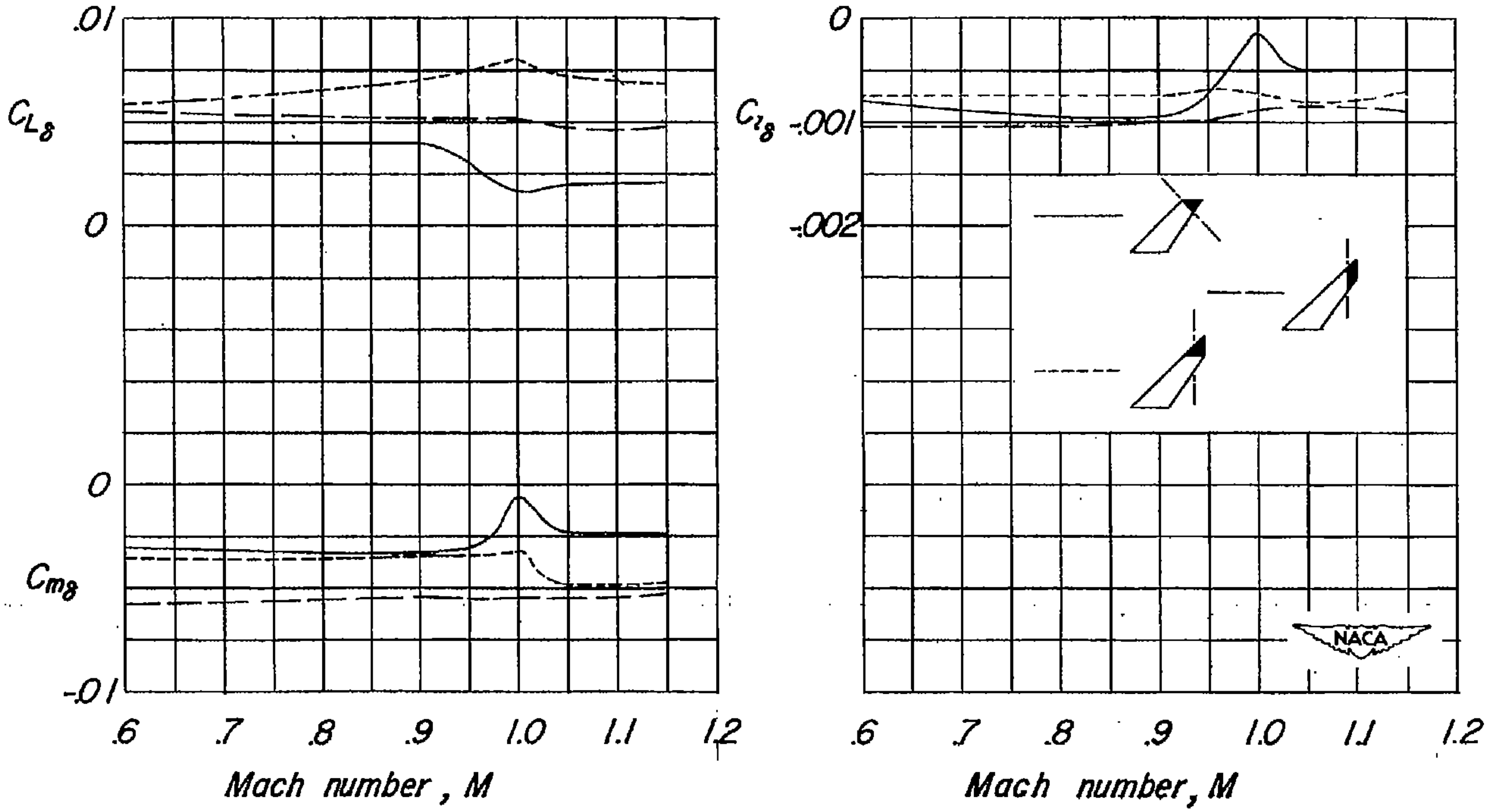

Figure 10.- The variation of the control parameters C_{L_δ}, C_{m_δ}, and C_{l_δ} with Mach number for three wing-tip ailerons investigated on a 51.3° sweptback wing. $\alpha = 0^\circ$.